

KWR 2015.097 | December 2015

Effects of small scale eolian activity on soil and vegetation of grey dunes



Effects of small scale aeolian
activity on soil and vegetation of
Grey dunes

Effecten van kleinschalige
verstuiving op bodem en vegetatie
van Grijze duinen

KWR 2015.097 | December 2015

Project number

400911

Project manager

Drs. Martin de Haan/ Dr. Edu Dorland

Client

DPWE

Quality Assurance

Prof. Dr. Pieter Stuyfzand

Author(s)

Dr. Y. Fujita & Drs. C.J.S. Aggenbach, with
cooperation of K. Wilschut

Sent to

DPWE

Year of publishing
2015

More information

Yuki Fujita
T 030 60 69 707
E Yuki.Fujita@kwrwater.nl

PO Box 1072
3430 BB Nieuwegein
The Netherlands

T +31 (0)30 60 69 511
F +31 (0)30 60 61 165
E info@kwrwater.nl
I www.kwrwater.nl



KWR 2015.097 | December 2015 © KWR

All rights reserved.

No part of this publication may be reproduced, stored in an automatic database, or transmitted, in any form or by any means, be it electronic, mechanical, by photocopying, recording, or in any other manner, without the prior written permission of the publisher.

Contents

Contents	3
1 Introduction	7
1.1 Background	7
1.2 Research questions	7
2 Methods	9
2.1 Sampling location	9
2.2 Soil sampling	16
2.3 Soil analysis	17
2.4 Vegetation recording	18
2.5 Geographical analysis	19
3 Results	21
3.1 Size and Ca content of deflation zone	21
3.2 Soil profiles on transects and within deflation zone	22
3.3 Soil chemical characteristics of NE transects	31
3.4 Spatial distribution of soil chemical properties	34
3.5 Vegetation	42
4 Synthesis of results	46
4.1 Effects on base chemistry of the top soil	46
4.2 Effects on vegetation	48
4.3 Conclusion	49
5 References	52
Appendix I XRF measurements	53

Samenvatting

Context onderzoek

Duinwaterbedrijven hebben een grote opgave voor het beheer en herstel van droge duingraslanden (habitattype Grijze duinen), zowel vanuit nationale regelgeving (Programmatische Aanpak Stikstof; PAS) als EU-regelgeving (Natura 2000). De afgelopen decennia is de ecologische kwaliteit van deze graslanden afgenomen: ze vergrassen en er treedt struweelvorming op. Daarom is in 2012 binnen het DPWE onderzoeksprogramma een meerjarige onderzoekslijn gestart naar de mogelijkheden voor ecologisch herstel van Grijze duinen. Dit onderzoek richt zich op de invloed van processen in de bodem, atmosferische stikstofdepositie en de effectiviteit van beheer- en herstelmaatregelen. Kleinschalige verstuiving door secundaire stuifkuilen wordt als een perspectiefvolle maatregel gezien voor behoud en herstel van Grijze duinen. Om die reden zijn komende jaren in het kader van de PAS veel maatregelen gepland om stuifkuilen met eolische activiteit te bevorderen. Tot voor kort was in de kustduinen weinig onderzoek verricht naar de ecologische effecten van kleinschalige verstuivingdynamiek. Daarom is in 2014 is DPWE-onderzoek gestart naar de effecten van kleinschalige secundaire verstuiving op de bodem en vegetatie van duingraslanden. Dit onderzoek keek naar de patronen en effecten van instuiving van zand in oud duingrasland rond 4 stuifkuilen die nog eolisch actief waren. In 2015 is soortgelijk onderzoek voortgezet in en rond 4 stuifkuilen die 14 tot 25 jaar geleden zijn gestabiliseerd.

Onderzoeksvragen

- Wat zijn de effecten van stuifzand op zuurgraad en geochemie van de bodem, humusprofiel en vegetatie, nadat stuifkuilen zijn gestabiliseerd?
- In hoeverre zijn kalkgehalte van het duinzand in de deflatiezone, mate van ontkalking van de omgeving bepalend voor deze effecten?
- Hoe groot is effect van voormalige verstuiving in ruimte en tijd op de duingraslanden?
- In welke mate kan kleinschalige verstuiving bijdragen aan een betere kwaliteit van habitattype Grijze duinen? Hoe verhoudt zich dat tot de ontkalkingsdiepte van het duinlandschap? En hoe lang zijn effecten van verstuiving op bodem en vegetatie aanwezig na stabilisatie van stuifkuilen?

Aanpak

Er werden twee stuifkuilen geselecteerd in relatief diep ontkalkt duingebied in de Luchterduinen en twee stuifkuilen ondiep ontkalkt duingebied in Meijndel. Van elke stuifkuil werden de bodemprofielen (humus, pH, kalk) beschreven op locaties in de voormalige deflatiezone en in 8 transecten gelijkmatig verdeeld over de windrichtingen in het omliggende duingrasland. Bij elke stuifkuil werd in één transect aan de zijde met de sterkste invloed van instuivend zand (NO of O) tevens bodemonsters genomen voor bepaling van het Ca-gehalte en werd de vegetatie beschreven.

Resultaten

In het duingrasland rond de onderzochte stuifkuilen heeft instuiving van kalkhoudend zand geleid tot een hogere basenrijkdom en pH van de

bodemtoplaag dan in de ontkalkte situatie voor de eolische activiteit. De effecten strekken zich uit tot een afstand van 10 tot 80 m vanaf de deflatiezone. De verhoging van de pH in de bodemtoplaag is het sterkst in de zone NO tot ZO van de deflatiezone, hetgeen samenhangt met de invloed van de overheersende windrichting. Het ruimtelijke effect verschilt tussen de afzonderlijke stuifkuilen. Deze verschillen hangen niet samen met verschillen in omvang van de voormalige deflatiezones (die verschillen weinig). De relatieve oppervlakte van het beïnvloedingsgebied (t.o.v. oppervlakte deflatiezone) vertoont een positieve relatie met het kalkgehalte in de deflatiezone. Variatie in de tijdsperiode tussen stabilisatie van de deflatiezone en het moment van deze studie kan ook invloed zijn geweest. De stuifkuilen in Meijndel, die groter beïnvloedingsgebied hadden, waren korter geleden gestabiliseerd dan die in de Luchterduinen. Daarnaast kunnen deze verschillen in beïnvloedingsgebied kunnen samenhangen met de geomorfologie van de stuifkuilen: hoe dieper de stuifkuil is uitgestoven, hoe groter het ruimtelijke effect was op de basenchemie van de bodemtoplaag.

De soortensamenstelling van de vegetatie in de deflatiezone wekt duidelijk af van die in de omgeving als gevolg het jonge successiestadium, het hogere kalkgehalte en de hogere pH van de bodemtoplaag. Hierdoor was het aandeel van soorten van basenrijk, voedselarm pioniervegetatie en basenrijk, voedselarm duingrasland hoger. In de transecten aan de NO- of O-zijde hadden deze soorten ook een hoger aandeel dichtbij de deflatiezone. In deze transecten gaat een sterke afname van de bedekking van basenminnende soorten samen met een sterke afname van de pH in de bodemtoplaag.

Geconcludeerd kan worden dat de basenchemie en vegetatie van duingraslanden in een zone van 10 tot 80 meters rond de stuifkuilen 14 tot 25 jaar na stabilisatie nog steeds duidelijk worden beïnvloed. Om deze reden is (re)activatie van stuifkuilen en achtereenvolgende stabilisatie een geschikte maatregel voor behoud en herstel van basenrijke duingraslanden. Wanneer de periode van eolische activiteit en de duur van stabilisatie worden opgeteld bedraagt de 'overlevingstijd' van basenrijk duingrasland minstens ca. 3 tot 5 decennia. (Re)activatie van stuifkuilen kan daardoor op een middellange termijn negatieve effecten van ontkalking en verzuring tegengaan. Dit geldt ook voor ontwikkeling van basenrijk duingrasland in de gestabiliseerde (re)activering van stuifkuilen (de kalkgehalte van het duingebied) en vermoedelijk ook de omvang van zandverplaatsing zijn bepalend voor de ruimtelijke omvang van de effecten op de basenchemie en soortensamenstelling van de vegetatie. De kwantitatieve invloed van zulke factoren op de ruimtelijke omvang en duurzaamheid van effecten kan nader worden bepaald op basis van een uitgebreidere analyse van de beschikbare data.

Preface

Water companies which produce tap water in Dutch coastal dunes are also important nature managers in these areas. Therefore they have a large responsibility for management and restoration of the habitat type H2130 Grey dunes (dry dune grasslands) in the Netherlands, and even in Europe. This habitat type is protected by the Habitat Directive of the EU. Last decennia the area and ecological quality of this habitat has declined due to grass and shrub encroachment, and eutrophication + acidification by atmospheric deposition. Coming years an extra effort in management is needed in the Netherlands because of a national program which counteracts the negative effects of a high atmospheric nitrogen load on nature (Programmatiese Aanpak Stikstof; PAS).

Since 2012 ecological research in the DPWE program of the coastal water companies focus on possibilities for restoration of Grey dunes and studies related soil factors and the effects of atmospheric N deposition. In 2014 research was conducted on the effects of blowouts with aeolian activity on the quality of dune grasslands (Fujita & Aggenbach 2015). This report documents the results of new research conducted in 2015 on the patterns of the soil and vegetation of Grey dunes of stabilized secondary blowouts. A more thoroughly interpretation of the results is foreseen in 2016. The refined results will also be used for management guidelines for (re)activation of secondary blowouts as measure for preservation and restoration of Grey dune habitat in a running OBN research (2015-2017).

We want to thank student Karin Wilschut, who was involved in the data collection and lab work for the research in 2015.

1 Introduction

1.1 Background

Blowouts play an important role in dune ecosystems to drive and maintain their dynamic development. Thick sand deposition from blowouts resets the succession, and stabilization of the blowouts by regeneration of dune vegetation initiates a new start of dune succession. On top of it, drift sands from blowouts also influence soils and vegetation of the surrounding dune ecosystems. Calcareous-rich drift sand from blowouts is considered to have positive effects on adjacent dune grasslands, especially those acidified due to natural decalcification and acidifying atmospheric deposition, since it improves base status of the soils. It may also counteract negative effects because of eutrophication by a high atmospheric nitrogen deposition. Even small-scale blowouts could have a positive effect on a vast area, when present at a certain density in space and time.

There have been a few studies which investigated ecological effects of small-scale blowouts on dune ecosystems. *Fujita and Aggenbach* [2015] examined effects of four, active, small blowouts in middle dunes and inner dunes, and found that the blowouts had significant effects on soil base status (i.e. higher soil pH, higher content of calcium carbonate, higher base saturation) and vegetation (i.e. more plant species adapted to base-rich conditions) in surrounding dune grasslands. The magnitude of the effects differed depending on multiple factors, such as the quantity of drift sand (i.e. size of the deflation area, distance and direction from the blowouts), geochemistry of the drift sand (i.e. calcium carbonate content), decalcification depth and base status of the background soil substrate, as well as soil organic matter content of the soil. The four blowouts that *Fujita and Aggenbach* [2015] examined have been active for the last decades (at least more than 40 years), whereas the majority of blowouts found in Dutch coastal dunes have a shorter active period or had been stabilized in last decades. A question is whether such difference in history of blowout has consequence in their influence on the surrounding dune vegetation. For this reason in 2015 4 stabilized blowouts were investigated for their effect on the surrounding dune grassland.

1.2 Research questions

This research aims at clarifying the effect of small-scale blowouts on surrounding dune soils and vegetation. Our particular focus is on blowouts which had been active for a long term but have been stabilized in the last decades. The research questions are:

- What are the effects of drift sands from stabilized blowouts on soil pH, humus profile, soil geochemistry, and plant species composition of surrounding dune grasslands?

- Which factors (e.g. calciumcarbonate content of the deflation zone, level of decalcification in the surrounding area) influence the magnitude of the effects?
- How large is the spatial and temporal effect of the blowouts on the surrounding dune grasslands?
- To what extent can small-scale blowouts contribute to improve quality of grey dune habitats? On which decalcification depth of the old dune grasslands? How long do the effects of the drift sand on soil and vegetation remain after stabilization of the blowouts?

It was not possible to address the last question in the research project of 2015 .In addition, this research will provide information on the effects of blowouts that were already stabilized, which contrasts with the presently active blowouts investigated by *Fujita and Aggenbach* [2015]. These results will be more extensively and synthetically analysed in a DPWE research in 2016 (when granted) and OBN research during 2015-2017 (Aggenbach et al. in prep) to elucidate how long a small-scale blowout remains effective for the conservation of the surrounding Grey dunes.

2 Methods

2.1 Sampling location

The field survey was conducted in four blowouts in coastal dune areas in the Netherlands, of which two locate in Meijendel area and the other two in Luchterduinen area (Figure 1). The blowouts have contrasting calcium carbonate richness and levels of decalcification depth in the surrounding areas (Table 1). The selection of the blowouts was based on the aerial photos of multiple years (2011, 2006, 2001, 1990, 1979, and 1968 for Luchterduinen; 2009, 2001, 1995, 1990, 1985, 1980, 1962, 1938 for Meijendel). The blowouts were selected with the following criteria: 1) the blowout is stabilized for 10 to 20 years, and 2) before the stabilization the blowout was active for at least 20 years. See Figure 3 for the changes in blowout extension, interpreted from the aerial photos in the past. In addition, it was checked that the blowout has a diameter of more than 20 m when it was active, and were surrounded by grasslands during the past 35 years. Also, none of the blowouts was close to the coast (>1.5 km) in order to prevent effect from sand transport from the beach and coastal sand. We tried to select blowouts which do not have other large blowouts nearby, especially in the direction of prevailing wind. This criterion could not be fully fulfilled: blowout 2 has two other blowouts in the surroundings, ca. 50 m away on the South-East side and ca. 20 m away on the South side. In the field, we also checked that the surrounding areas (especially at the NE and O site) of the selected blowouts were not on a steep slope and not disturbed by animals (particularly rabbits) or water erosion.

At each blowout, we established four transects: one runs parallel to the prevailing wind direction (i.e. south-west to north-east; Figure 2) and crosses the broadest zone with former sand deposition (northeast site), another runs perpendicular to this (i.e. north-west to south-east), and the other two run in between (i.e. south to north and west to east). Note that, for blowout 8, the transect running to east direction was considered as the transect with the strongest influence of sand deposition. Photos of transects to north-east or east direction are shown in Figure 4. Since we are primarily interested in the effect of sand deposition on dune grasslands, we adjusted the exact direction of the transect in the field so as not to run across shrubs or woodlands. We stretched the transects up to the point where the influence of the blowout becomes not evident in terms of visible recent sand deposits in the soil profile (i.e. no fresh sand layer on a humus layer) and calcium carbonate- and pH-profile of the soil with deeper decalcification and stronger acidification.

Table 1. Characteristics of four sampling locations around a blowout.

Blowout number	Area	Dune type	Time (years) after stabilization ^{*1}	Active period (years) before stabilization ^{*1}	Blowout most active in ^{*1}	CaCO ₃ -richness of blowout ^{*2}	Decalcification depth of surrounding area (cm below surface) ^{*3}	Distance to the sea (ca. km)
2	Meijendel	Middle dune ^{*4}	6-14	16-29	1990	relatively rich	15 - 20 cm	1.5 km
8	Meijendel	Inner dune	6-14	15-39	1990	moderate	19 - 22 cm	2.6 km
16	Luchterduinen	Inner dune	14-25	>11	1990	moderate	40 - 80 cm	4.0 km
21	Luchterduinen	Middle dune	ca. 25	15-20	1979 or earlier	relatively rich	30 - 60 cm	2.1 km

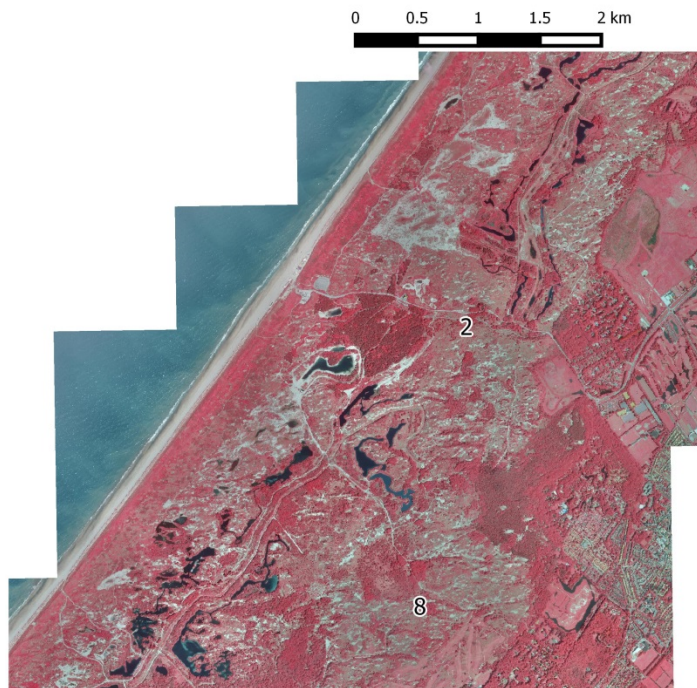
^{*1}: Approximated from multiple aerial photos from the past

^{*2}: primarily judgement derived from position in dune landscape zonation

^{*3}: calcification depth indicative; data from decalcification map Luchterduinen and some soil profiles. Decalcification depth is assessed in soil profiles as the boundary between no fizzle and fizzle after dripping the soil with 10% HCl solution.

^{*4}: On the boundary of middle dune and inner dune

Meijendel



Luchterduinen



Figure 1. Location of two blowouts in Meijendel (2 and 8, top) and two blowouts in Luchterduinen (16 and 21, bottom). Aerial photos of 2009 (for Meijendel) and 2011 (for Luchterduinen) are shown background.

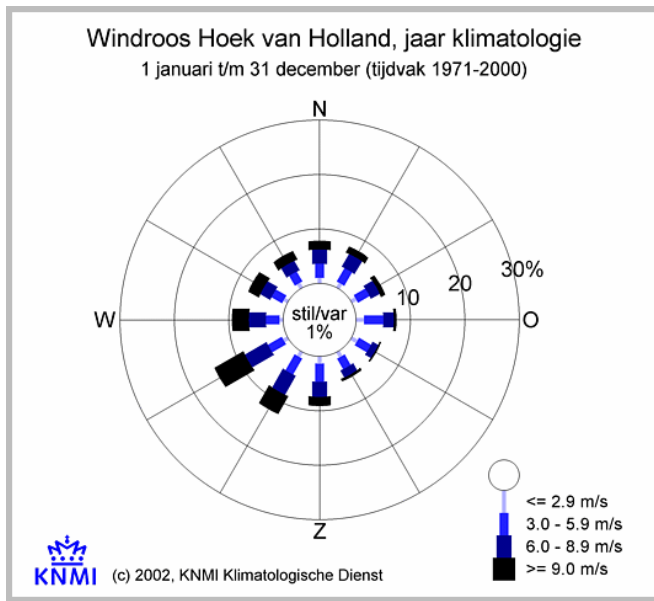
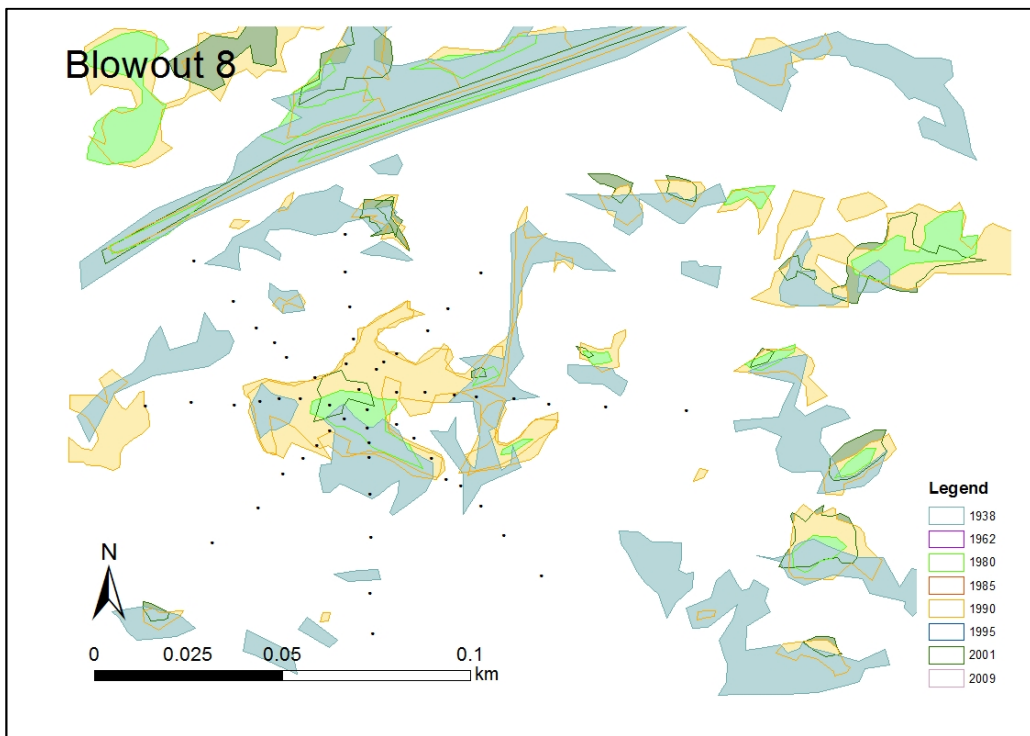
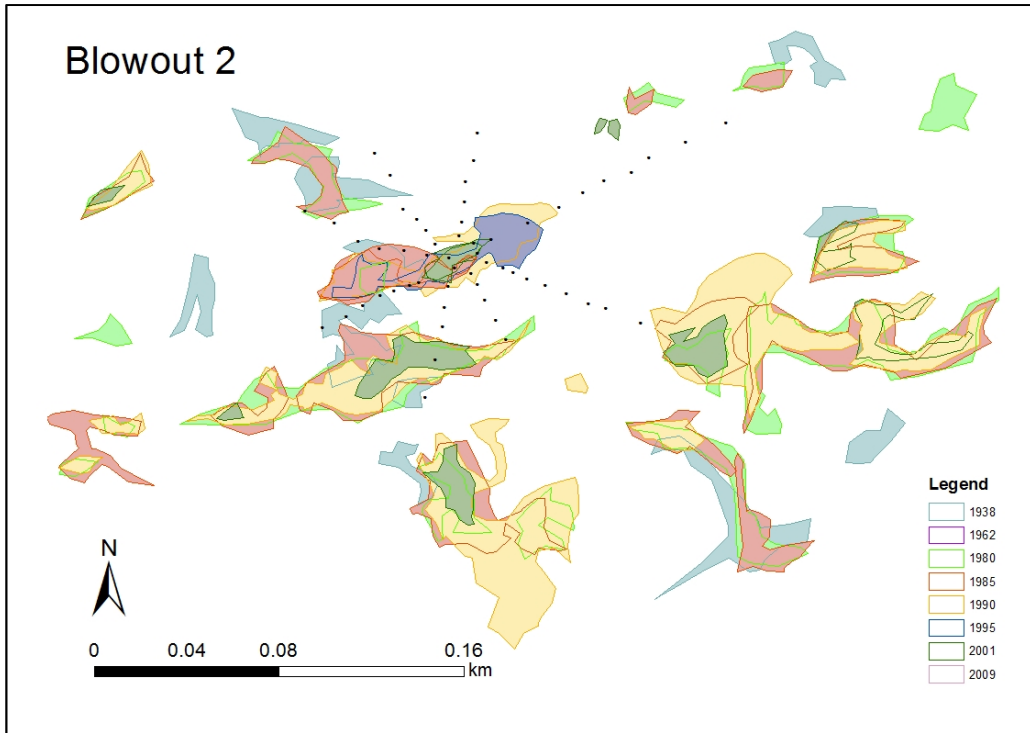


Figure 2. Prevailing wind direction in Hoek van Holland (KNMI 2002)



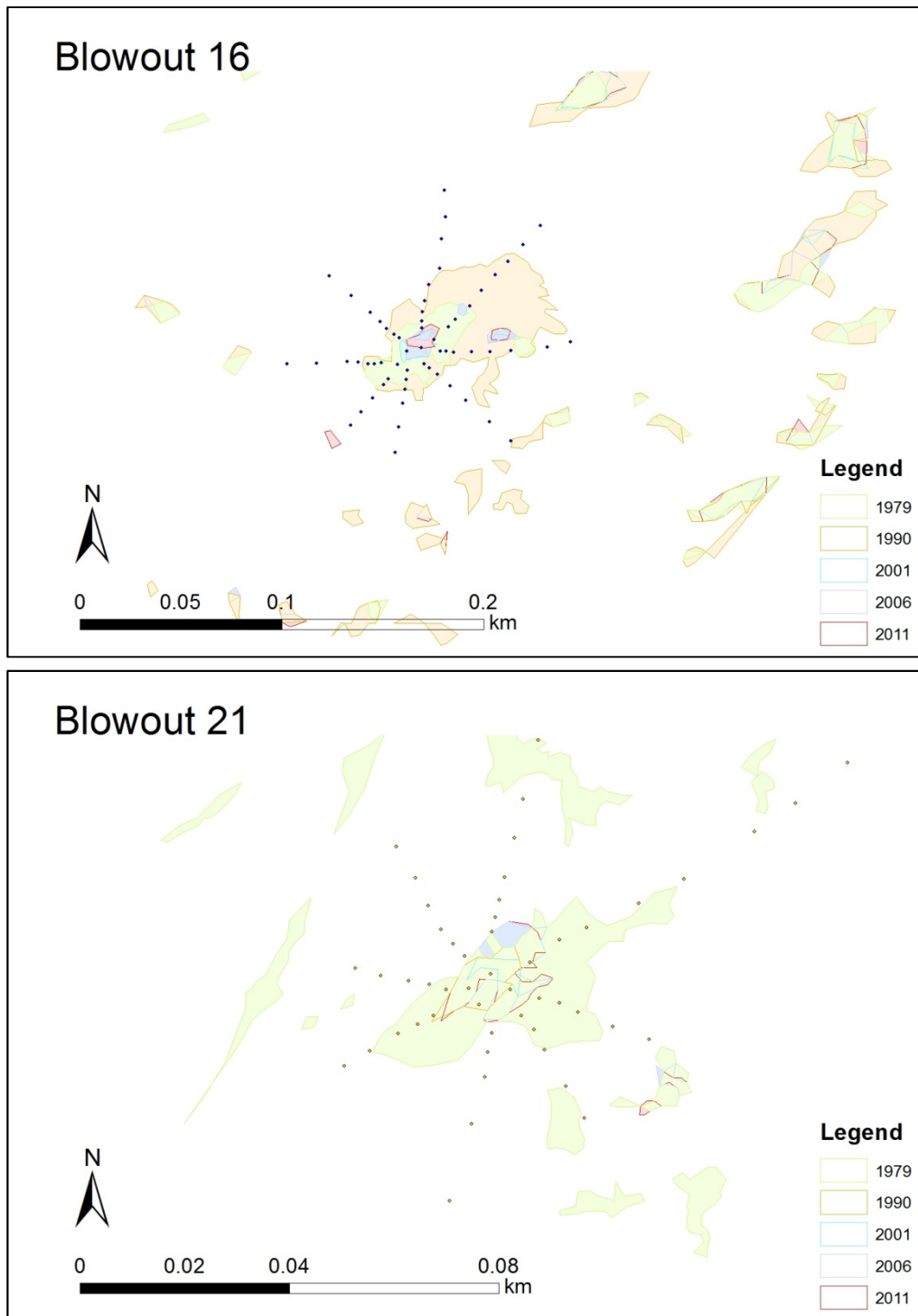


Figure 3. Spatial changes in blowouts in the past. The extension of blowouts was interpreted from aerial photos of multiple years. Dots are the locations of plots of this study.

Meijendel blowout 2

Deflation zone in NW-direction



NE transect in E-direction



Meijendel blowout 8

Deflation zone in NW-direction



E transect in E-direction



Luchterduinen blowout 16

Deflation zone



NE transect in NE-direction



Luchterduinen blowout 21 Deflation zone in ZW direction



NE transect in NE-direction



Figure 4. Photos of the deflation zone and the transect with the strongest effect of former sand deposition of the four blowouts. Photos were made in april 2015.

2.2 Soil sampling

In April 2015, on each transect, we sampled soil profiles down to ca. 30 cm depth with a 'humushapper', at the interval of ca. 3-10 m between sampling points (see Figure 5 for the layout of the sampling points). In the intensive transect with supposed strong effect of sand deposition with a Edelman auger profiles were sampled down to 120 cm depth. At locations near the deflation zone in other transect with the profiles were taken until the buried older humus profile was reached or until 120 cm depth. For each soil horizon, we recorded the horizon type according to *Van Delft* [2004]. Additionally we distinguished the thickness of the living moss layer, and horizons with dead moss. For graphical presentation purpose, the soil horizons were further grouped into 5 categories: living moss, dead moss, fresh to slightly decomposed litter (L+F), organic-rich sand (Ah), sand with moderate amount of organic matter (AC), and organic-poor sand (C). We also estimated calcium carbonate richness by dropping 10% HCl solution. We distinguish three classes of calcium carbonate richness: K0: no fizzing (no CaCO_3), K1: weak fizzing visible or audible (moderate CaCO_3), K2: strong fizzing visible (high CaCO_3). With this method, decalcification depths up to 120 cm were obtained for each location by using both the humushapper profile and as well using a Edelman soil auger. The decalcification depth was defined as the depth of the top of the first layer with class K1 or K2. Soil pH was measured in situ pH with a pH meter (Hanna H199121). When dry, the soil was wetted with MilliQ (very mineral poor water) in order to have pore water at positions for measurement. Depth of the pH measurements was done at regular intervals of 2.5, 5.0, 7.5, 10, 15, 20, 25, 30 cm below the top of the mineral profile. In order to carry out the pH profile measurements quickly measurement depth were not adjusted to the depth of humus and calcium carbonate profile. Soil pH was measured before dripping HCl for the calcium carbonate profile.

On the north-east transect of each blowout, we selected four points for extra soil measurements. Here soil samples were taken from 0-5 cm, 5-10 cm, 10-15 cm, 15-20 cm, and 20-25cm depth. For each soil layer, ca. 100 g fresh soil was sampled, stored in a plastic 100 ml container and kept in fridge for chemical analysis in the lab. Another set of soil samples was taken for the same 5 layers with a metal ring (diameter 67.3mm) for bulk density estimate.

In addition, within the deflation area of each blowout, soil samples were taken from 4 points for the depth of 0-5 cm, 5-10 cm, 10-15 cm, 15-20 cm, and 20-25 cm depth. The soil samples were stored in fridge for chemical analysis in the lab. Similar 4 soil samples were taken with the metal ring (diameter 67.3mm) for bulk density estimate for the same depths.

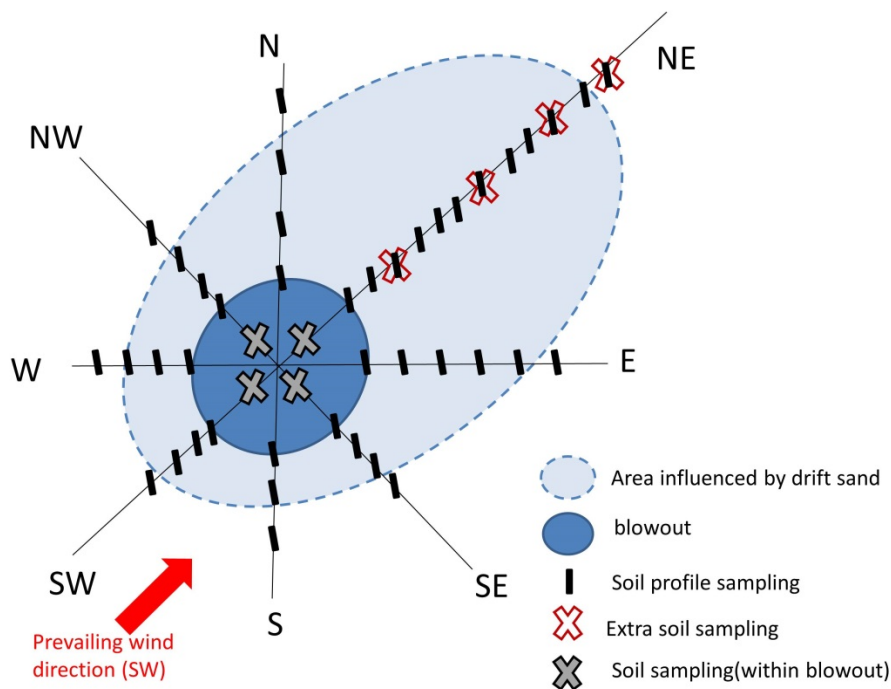


Figure 5. Configuration of four transects around a blowout and sampling points.

2.3 Soil analysis

Bulk density was estimated for all soil samples by measuring the weight after drying at 65° C for 48 hours. Soil chemical analysis was conducted for the top 3 depths (0-5 cm, 5-10 cm, and 10-15 cm) only. The soil samples were homogenized after removal of visible roots and living mosses were removed and sieved with a 2 mm sieve, and split into subsamples for further analysis. With sieving no shell fragments were removed. pH_KCl and pH_H2O were measured with a pH meter (Hanna H199121) after mixing ca. 10 g of the field moist soil with 25 ml 1M KCl solution and with 25 ml demineralized water, respectively, and shaking for two hours. Moisture content of soil was determined after drying at 105 ° C for 48 hours.

Total amount of elements were estimated with a handheld X-ray fluorescence (XRF) analyser (NITON XL3t GOLDD). XRF measures 30-40 elements (including Al, Ca, Fe, Mg, Mn, P, S, Sr and Ti) non-destructively. Prior to the analysis, we have tested whether the XRF can accurately estimate the total amount of elements, by using a selection of 103 mineral soil samples taken from a OBN study on the geochemistry of sand deposits of foredune areas of the Dutch coastal dunes [Stuyfzand *et al.*, 2012]. Total element concentrations in these samples had been analysed by ICP-OES of HF-extracts. We selected samples originating from sites which were not affected by eolian sedimentation of sand originating from coastal sand suppletion. The samples covered the range of CaCO₃, titanium and soil organic matter content which are typical for coastal dune ecosystems. The test analysis revealed that fine grinding is necessary prior to the XRF measurements to achieve reasonable repeatability of values in replicas for total Ca. Therefore, we used machine-ground soil samples to measure element concentrations with the XRF analysis for the 103

samples. In appendix I the comparison of concentrations of several elements (Ca, Sr, Al, Ti, Fe, Si) between those measured with ICP-OES and with XRF are shown. Linear regression analysis was conducted for each element to correct the XRF-measured the concentrations for the ICP-measured element concentrations (Appendix I).



Figure 6. Handheld XRF analyser (left) and soil samples (right)

For the XRF measurements of soils of this study, for each plot, soil samples were dried at 65 °C for 48 hours and machine-ground. A plastic cup (ca. 2.4 cm diameter), covered with a thin polypropylene film, was filled with the soil at least to 7 mm height. Measurement time was set to be 30 seconds per category of elements. Measurements were repeated twice by taking two subsamples for each soil sample. Each element was measured with the unit of ppm, which was converted to percentage by multiplying with 1/10000. In this report we only present total Ca-measurements. The Ca concentrations measured with XRF were corrected using the regression model of XRF-measured Ca concentration (Ca_{XRF}) and ICP-measured Ca concentration (Ca_{ICP}) obtained from test analysis with the soil samples of *Stuyfzand et al.* [2012]: $Ca_{ICP} = 0.7883 * Ca_{XRF} + 1627.8$ ($R^2=0.995$, $N=98$).

2.4 Vegetation recording

In June 2015 vegetation was recorded in the NE transects for all blowouts. A plot of 1m² was established next to the soil profile sampling points. Abundance of vascular plants, mosses, and lichens was recorded with Londo scale. Cover and height of vegetation was separately recorded for shrubs+ trees, herbs, and mosses+lichens.

Each species was categorized into one of 13 'ecological species groups' for dry dunes based on their syntaxonomical and abiotic preference [Aggenbach unpublished]. See Table 2 for the description of each ecological species group. For each plot, number of species and cumulative cover of these species were calculated for each group. Since some of the groups occurred only occasionally (i.e. group 1 (9% cumulative cover in all plots together), group 4 (0%), group 8 (1.5%), and group 13 (3.5%)), we clumped these minor species groups into 1 category for the graphical presentation in Figure 22 and Figure 23.

Furthermore, Ellenberg indicator values of acidity were retrieved from the database GermanSL for vascular plants and lichens, and from Siebel (2005) for mosses and weighted average values (weighted for cover of each species) were calculated for each plot.

Table 2. Description of ecological species groups

1: dry pioneer and field vegetation nutrient rich	8: Heath grasslands nutrient-poor weakly-buffered
2: dry pioneer vegetation nutrient-poor base-rich	9: mesophytic grassland moderately nutrient-rich
3: dry pioneer vegetation nutrient-poor moderate base-rich	10: grassland nutrient-rich
4: dry pioneer vegetation nutrient-poor base-poor	11: dry forest edge and forb vegetation base-rich
5: dry dune grassland nutrient-poor	12: shrub and forest
6: dry dune grassland nutrient-poor base-rich	13: indifferent and unknown
7: dry dune grassland nutrient-poor base-poor	

2.5 Geographical analysis

2.5.1 Plot geometry

The boundaries of the former deflation areas were mapped in the field using RTK-GPS (accuracy ± 0.02 - 0.03 m), judged from the local topography. The area of the deflation area was computed using ArcGIS 10.1 Furthermore, for each plot, distance between the plot and the boundary of the deflation area was calculated using ArcGIS 10.1.

2.5.2 Mapping influence of blowouts

In-situ pH values of 2.5 cm depth and 10 cm depth in sampling points on four transects (SW – NE, NW – SE, S-N, and W-E) were linearly interpolated onto a grid using the algorithm of Akima [Akima, 1978], using the package 'akima' of statistical program R. Consequently, based on the grid values, contour maps were drawn.

For each sampling point, change in in-situ pH within 0 to 10 cm depth was calculated with linear regression analysis of the pH values available within the depth range. For majority (N=216 out of 221) of the sampling point, four pH values (2.5, 5, 7.5, and 10 cm depth) were used to derive the regression model. A negative slope of the regression model means that pH values are higher in top layers than deep layers, whereas a positive slope means that pH values are lower in top layers than deep layers. The slope values were linearly interpolated to draw contour lines. These maps were used to evaluate the pH-gradients in the topsoil.

Decalcification depth of each sampling point was computed as the middle depth of the shallowest soil layer where CaCO₃ was detected (i.e. 'K1' or 'K2' by in-situ HCl dropping method). The decalcification depth was linearly interpolated to draw contour lines.

Additionally, we have classified each sampling points into three categories of degree of influence by the blowout (i.e. 'strongly influenced', 'weakly influenced', and 'hardly influenced'). In principle, a point was classified as 'strongly influenced' if the top soil contains calciumcarbonate (judged by in-

situ HCl dropping method at 2.5 cm depth) or if the top soil in-situ pH is much higher (i.e. more than pH unit of 3) than the background pH. The background pH was approximated by the lowest in-situ pH value among all sampling points of the blowout site. A point was classified as 'weakly influenced' if the top soil in-situ pH is moderately higher (i.e. more than pH unit of 2) than the background pH. Soil humus profile information was also looked at to aid the judgement of the classification. Subsequently, we roughly drew the boundary of the zones which is strongly and weakly influenced, by connecting the eight transition points (from strongly to weakly influenced point, and from weakly to hardly influenced point) on the transects. Deflation area was excluded from the area calculation of influenced area. The area of each zone was calculated on ArcGIS.

3 Results

3.1 Size and Ca content of deflation zone

The area of former deflation zone was 347 m² for blowout 2, 260 m² for blowout 8, 397 m² for blowout 16, and 225 m² for blowout 21 (see Figure 20 for their spatial configuration). Generally the deflation zones of all blowouts were small. The deflations zones of blowout 16 and 21 were completely stabilized by vegetation. The other two were for a greater part stabilized, but a part of the deflation areas showed signs of weak eolian activity. In the Sourthern part of blowout 21 a patch of productive vegetation was developed due to influence of raising groundwater table in the rooting zone (as detected by aerial photos).

Calcium content of deflation zone was in general higher in Meijendel than Luchterduinen and in middle dunes than inner dunes. It was highest in blowout 2, followed by blowout 8, blowout 21, and blowout 16 (Figure 7). Note for the two Meijendel sites the Ca-content at 10-15 cm depth is different, while the two Luchterduinen have the similar range at this depth. In all blowouts, Ca content was higher in deeper soil layers compared to shallower soil layers, implying stabilization of the blowouts in the last decades. Standard errors of Ca were large especially in blowouts in Meijendel, indicating large spatial variations within the blowouts.

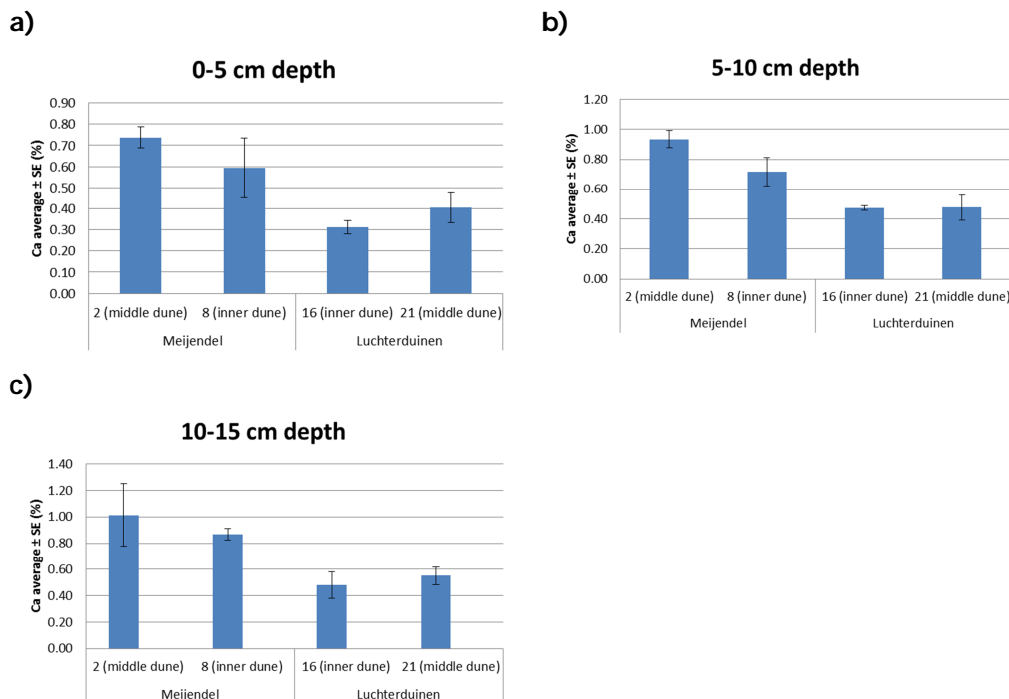


Figure 7. Total calcium content (% in dry weight) of soils in deflation zone at a) 0-5 cm depth, b) 5-10 cm depth, and c) 10-15cm depth, measured with XRF analyser (and corrected for ICP-measured concentrations: see Method). Average values and standard errors (N=4) are shown. 1% Ca content is equivalent to ca. 2.5 % CaCO₃, with an assumption that all Ca (m.w. 100.0869 g/mol).

3.2 Soil profiles on transects and within deflation zone

Profiles of-situ pH measurements, calciumcarbonate, and humus horizons are shown in cross sections for blowout 2 (Figure 8), blowout 8 (Figure 9), blowout 16 (Figure 10), and blowout 21(Figure 11).

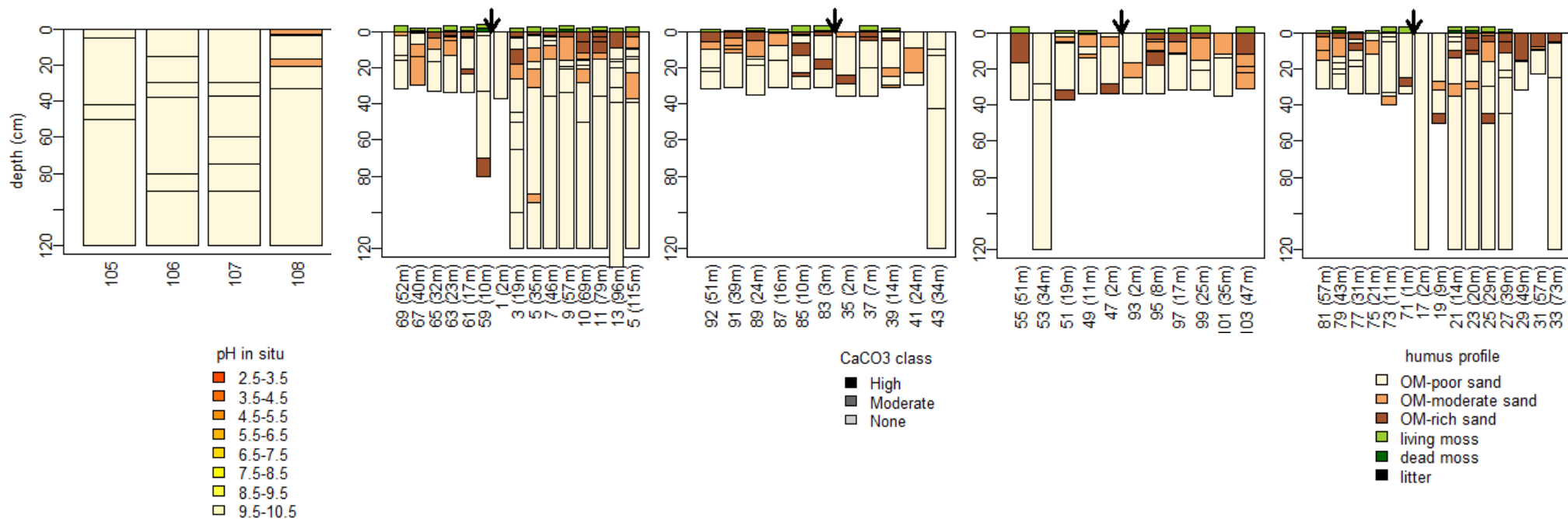
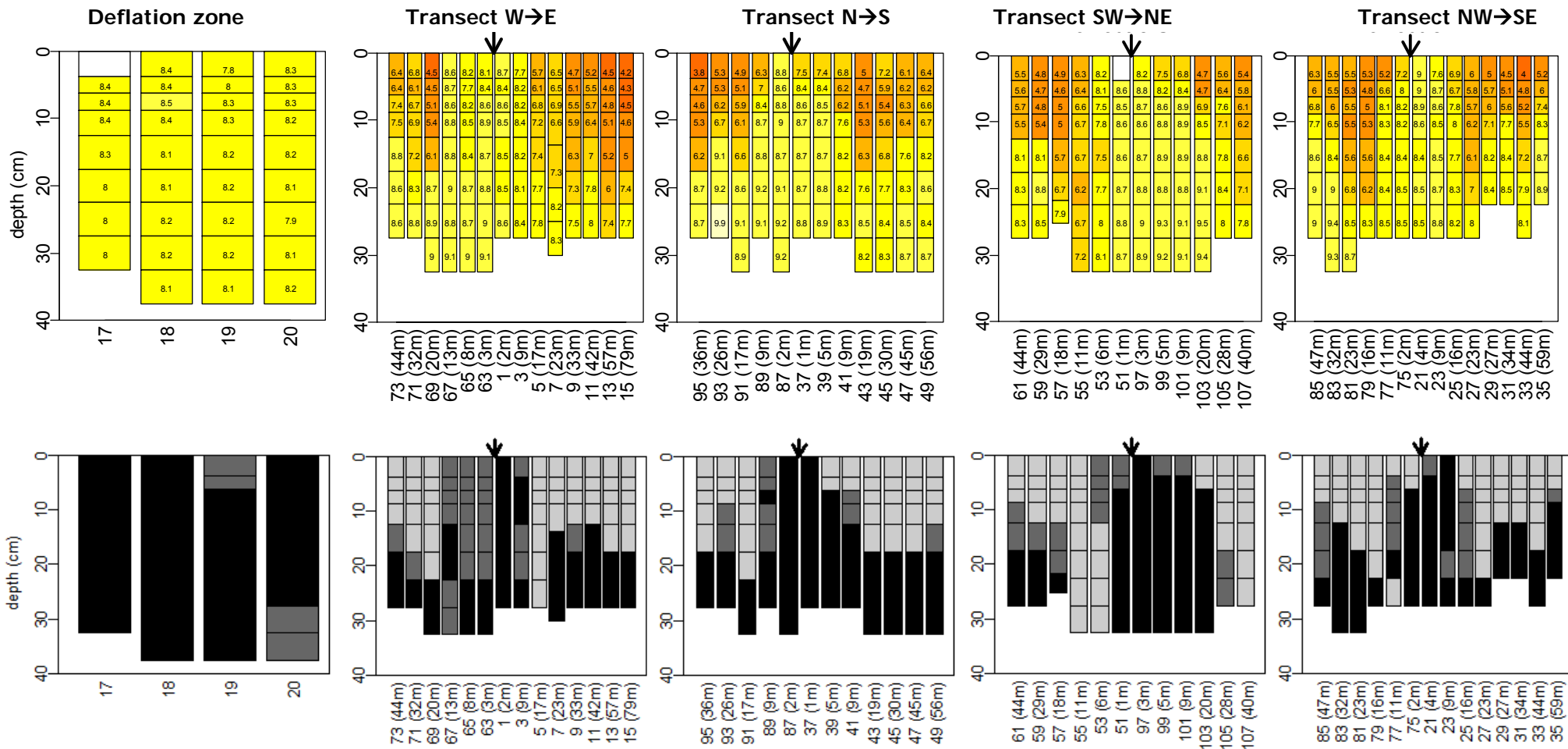


Figure 8. in-situ pH (top), CaCO₃ class (middle), and humus profile (bottom) of **blowout 2** in Meijndel, within deflation zone and for transect SW - NE, NW - SE, S-N, and W-E. For plots on transects, distance (m) between the plot and the boundary of the deflation zone is shown in bracket. Arrow shows the position of the deflation zone on each transect. For in-situ pH and calciumcarbonate class, blank cells with no value indicate that there are no data available for that depth.



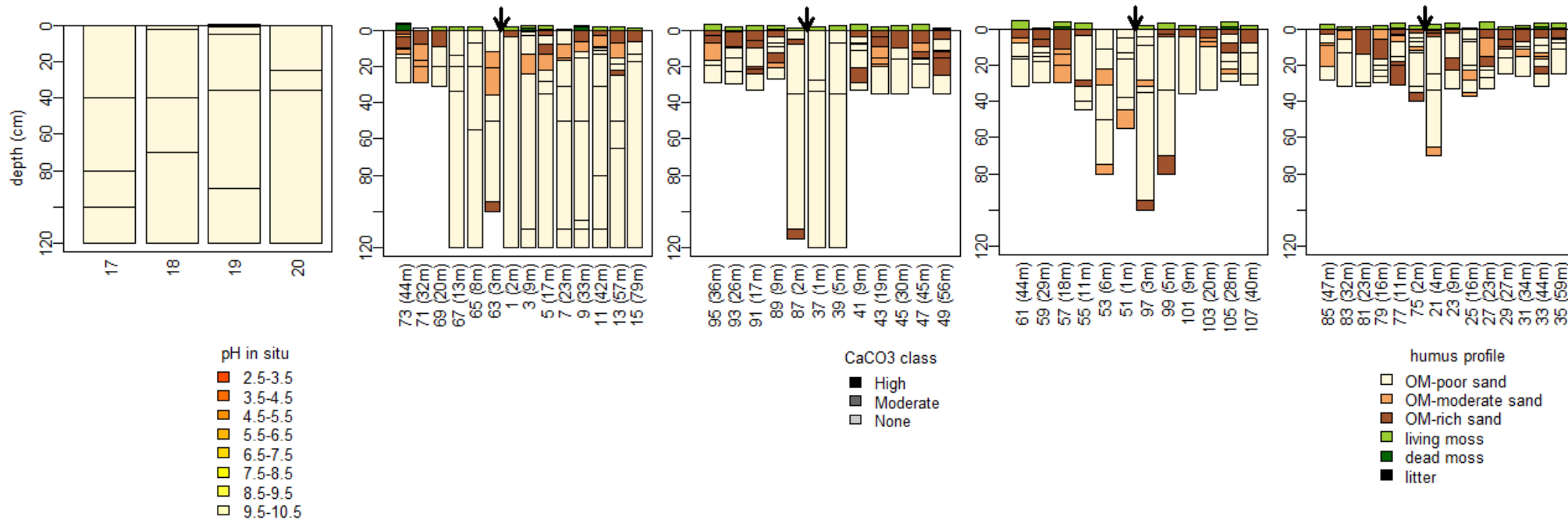
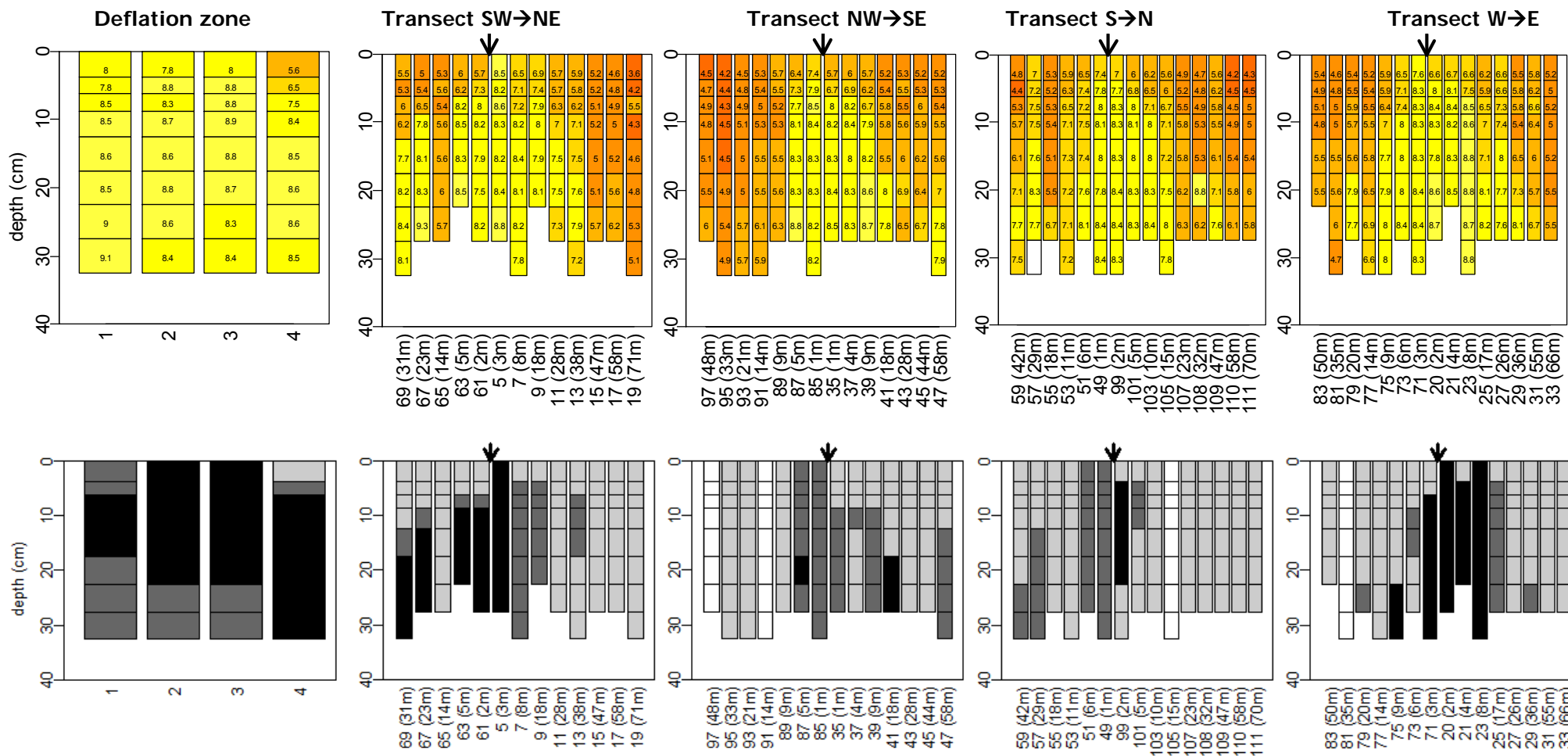


Figure 9. in-situ pH (top), CaCO₃ class (middle), and humus profile (bottom) of **blowout 8** in Meijendel, within deflation zone and for transect SW - NE, NW - SE, S-N, and W-E. For plots on transects, distance (m) between the plot and the boundary of the deflation zone is shown in bracket. Arrow shows the position of the deflation zone on each transect. For in-situ pH and calciumcarbonate class, blank cells with no value indicate that there are no data available for that depth.



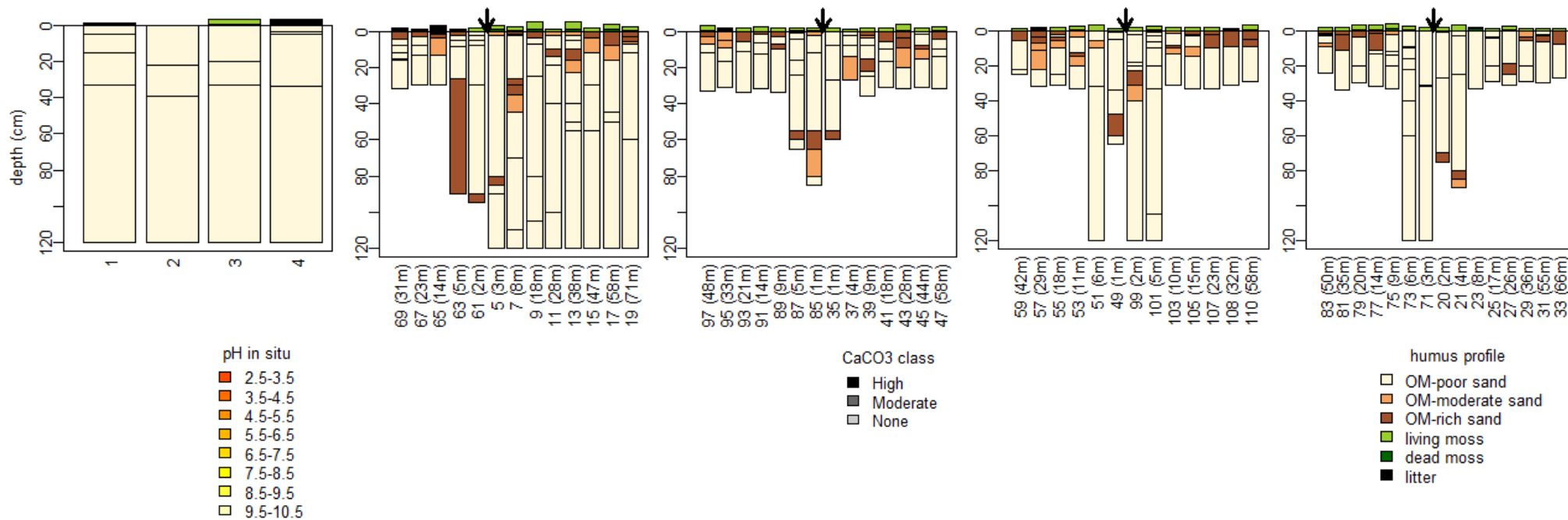
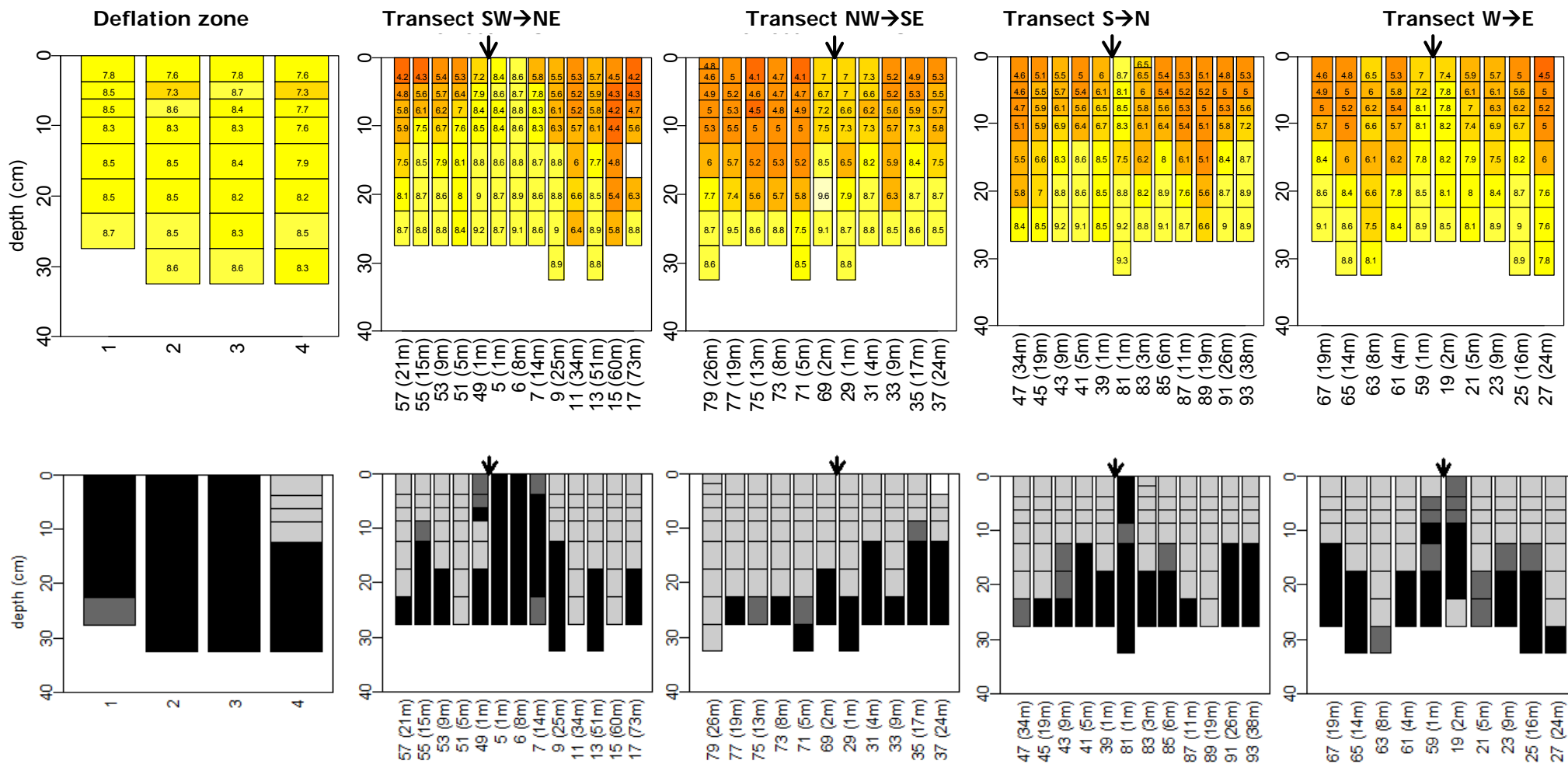


Figure 10. in-situ pH (top), CaCO₃ class (middle), and humus profile (bottom) of **blowout 16** in Luchterduinen, within deflation zone and for transect SW – NE, NW – SE, S-N, and W-E. For plots on transects, distance (m) between the plot and the boundary of the deflation zone is shown in bracket. Arrow shows the position of the deflation zone on each transect. For in-situ pH and calciumcarbonate class, blank cells with no value indicate that there are no data available for that depth.



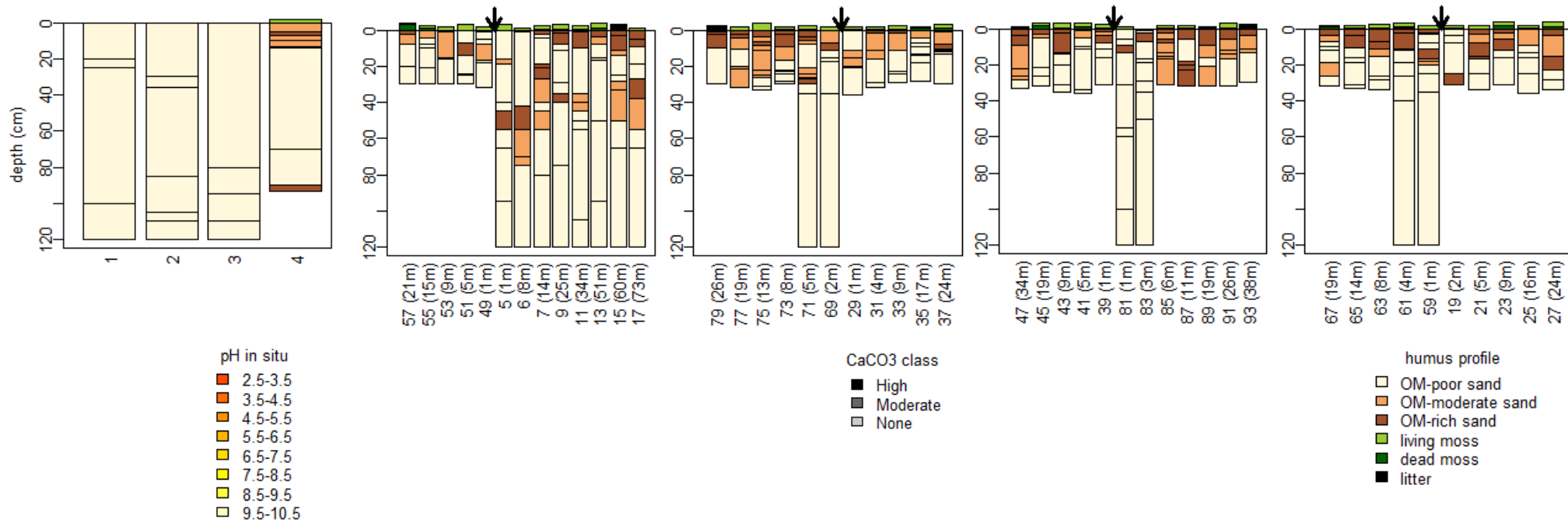


Figure 11. in-situ pH (top), CaCO₃ class (middle), and humus profile (bottom) of **blowout 21** in Luchterduinen, within deflation zone and for transect SW - NE, NW - SE, S-N, and W-E. For plots on transects, distance (m) between the plot and the boundary of the deflation zone is shown in bracket. Arrow shows the position of the deflation zone on each transect. For in-situ pH and calciumcarbonate class, blank cells with no value indicate that there are no data available for that depth.

3.3 Soil chemical characteristics of NE transects

For sampling points on the north-east transect, pH_{H₂O} (Figure 12), pH_{KCl} (Figure 13), total calcium content (Figure 14), and bulk density (Figure 15) are shown for each of the three sampling depths.

The pH-measurements in the deflation zone showed weak acidification of the topsoil. The top soil acidification was most evident in the deflation zone of blowout 16. The NE-transect of blowout 2 has the broadest zone with a high pH. The zone with relatively high pH-values has (slightly) lower pH in the 0-5 cm layer than the lower layers. Again this acidification was most evident in blowout 16. At the end of the transects pH-values were low in all three layers. Lowest values were recorded for blowout 8, followed by 16 and 21.

Ca contents were in general higher in deflation zone, and higher in lower soil layers than shallower layers (Figure 14). The spatial difference and depth difference were smaller in Luchterduinen (blowout 16 and 21) than in Meijendel.

Bulk density was in general lower in plots far from the deflation zones, and lower in top soil than in deeper soil layers (Figure 15). This reflects higher soil organic matter accumulation in these sampling points.

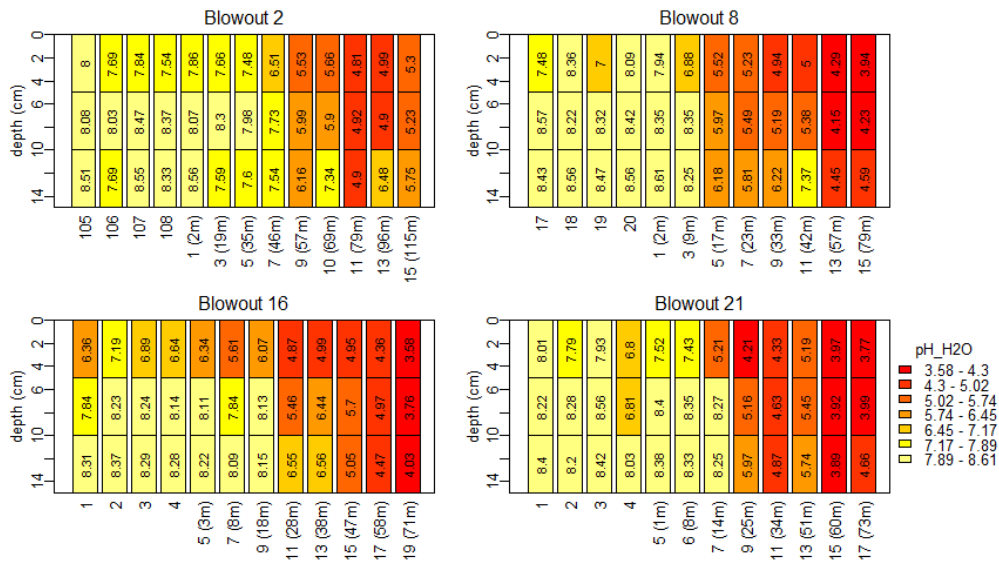


Figure 12. pH_{H2O} of soil layers 0-5 cm, 5-10 cm, and 10-15 cm depth for four blowouts. The four plots on the left side are within deflation zone. Rest of the plots are located at the NE transect, for which the distance between the plot and the boundary of the deflation zone are shown in bracket.

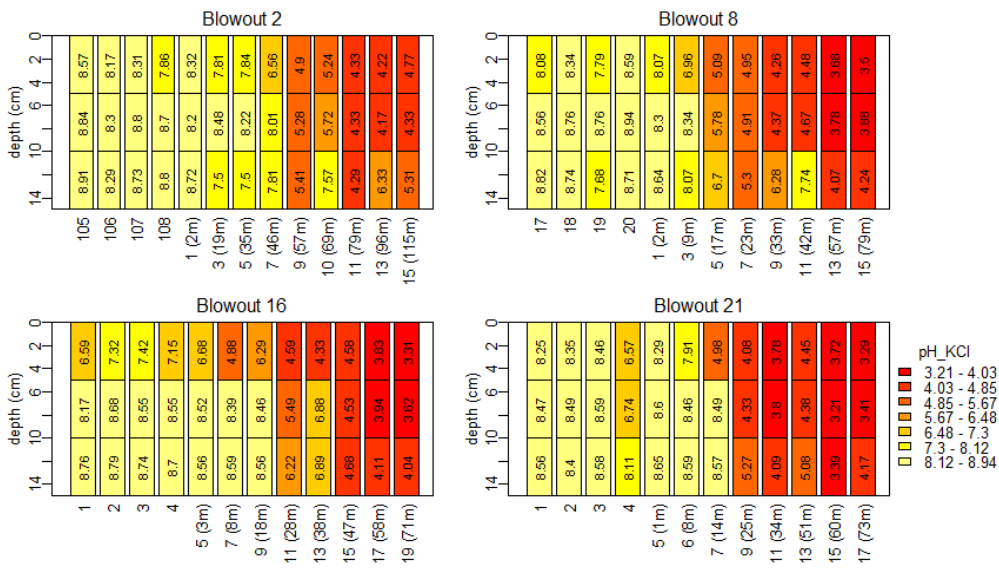


Figure 13. pH_{KCl} of soil layers 0-5 cm, 5-10 cm, and 10-15 cm depth for four blowouts. The four plots on the left side are within deflation zone. Rest of the plots are located at the NE transect, for which the distance between the plot and the boundary of the deflation zone are shown in bracket.

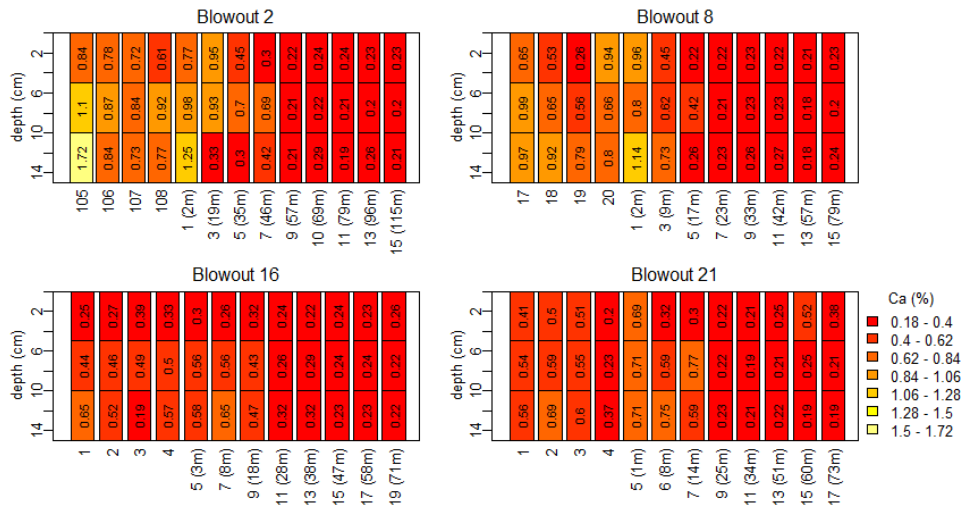


Figure 14. Total amount of calcium (%), measured with XRF analyser (and corrected for ICP-measured concentrations: see Method), in soil layers 0-5 cm, 5-10 cm, and 10-15 cm depth for four blowouts. The four plots on the left side are within deflation zone. Rest of the plots are on NE transect, for which the distance between the plot and the boundary of the deflation zone are shown in bracket. 1% Ca content is equivalent to ca. 2.5 % CaCO₃, with an assumption that all Ca (m.w.=40.078 g/mol) is present as CaCO₃ (m.w.=100.0869 g/mol).

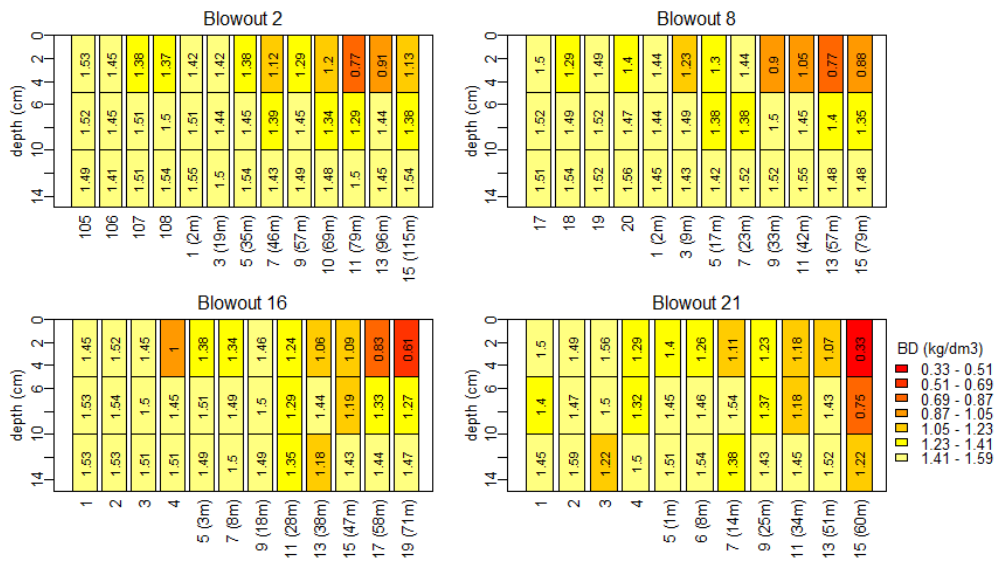


Figure 15. Bulk density (kg/dm³) of soil layers 0-5 cm, 5-10 cm, and 10-15 cm depth for four blowouts. The four plots on the left side are within deflation zone. Rest of the plots are located at the NE transect, for which the distance between the plot and the boundary of the deflation zone are shown in bracket. Because of a strong relationship between bulk density and soil organic matter (SOM) content, a low bulk density indicates a relatively high SOM-content.

3.4 Spatial distribution of soil chemical properties

3.4.1 In-situ pH at 2.5cm and 10cm depth

In-situ pH values of top soil (i.e. at 2.5 cm depth) were interpolated to show the spatial distribution of soil acidity around the blowouts (Figure 16). A large area around blowout 2 had a high pH in the top soil. Since the humus richness in top soil seems indifferent among blowouts (see humus profile and bulk density in earlier section), the higher pH values around blowout 2 compared to other blowouts is most likely caused by the drift sands from the blowout. For blowout 8, the extent of the area with high topsoil pH was smaller than that of blowout 2. For blowout 16 and blowout 21 only very small areas around the blowout had elevated pH in the top soil. At blowout 2 the zone with elevated pH around the deflation area is broadest at the SW, S and NE transect. At blowout 8 this area is more or less equally distributed around the deflation area. At blowout 16 and 21 this zone is broader at the NE transect.

In-situ pH values at 10cm depth shows similar pattern but for all blowouts the area with high pH's is larger (Figure 17). This is especially the case for blowouts 8, 16 and 21.

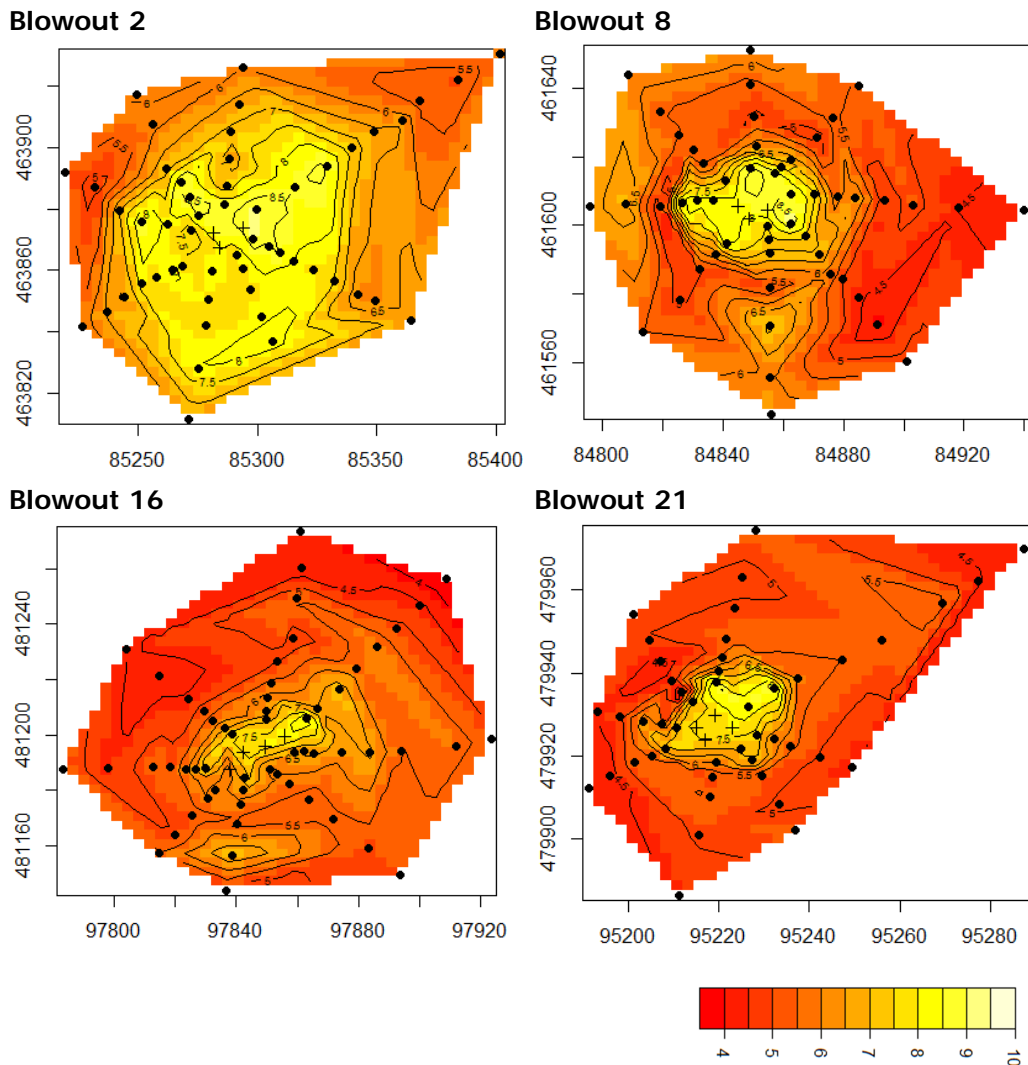


Figure 16. Contour map of in-situ pH of the top soil (2.5 cm depth), made by interpolation of point data from soil sampling locations. Dots are the sampling points on transects, and crosses are the sampling points within the former deflation zone. X and Y axis are X- and Y-coordinate in RD ('Rijksdriehoekskoördinaten') system (unit m).

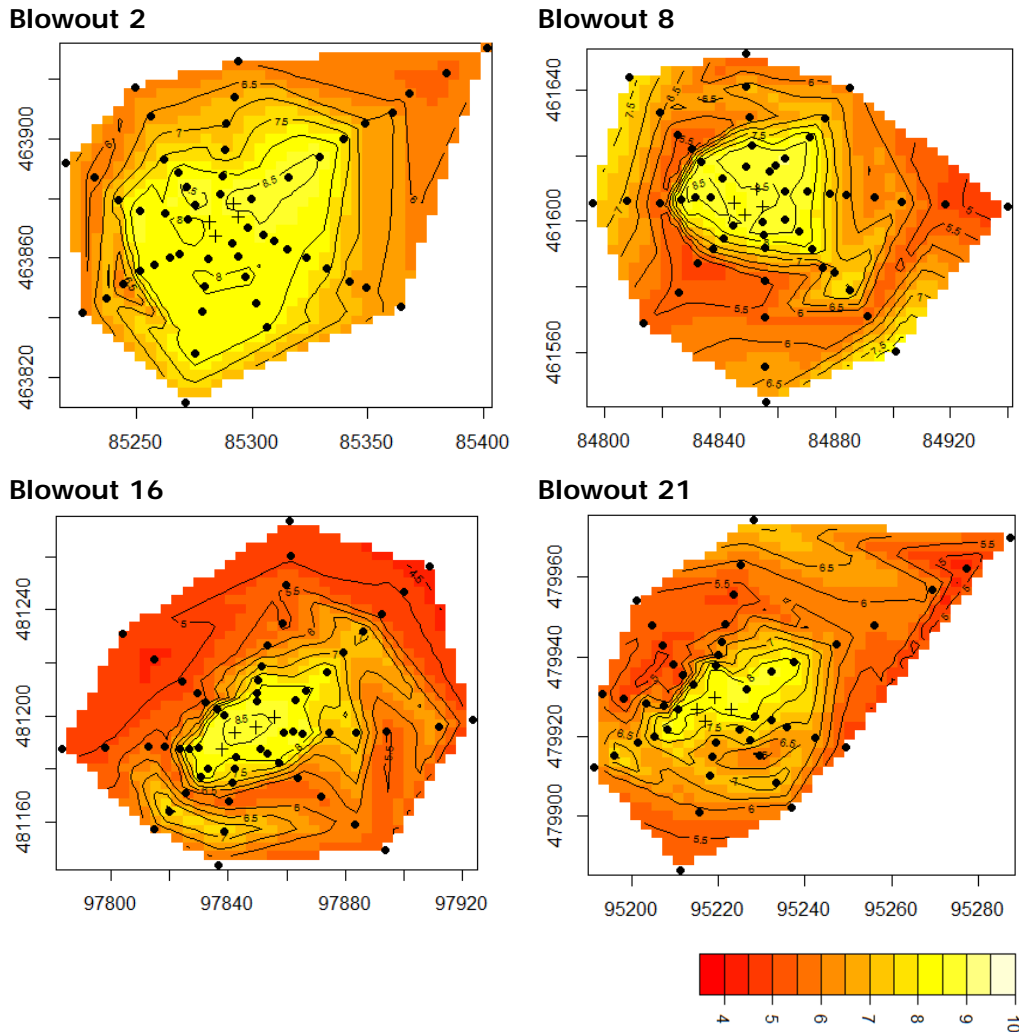


Figure 17. Contour map of in-situ pH of 10 cm depth, made by interpolation of point data from soil sampling locations. Dots are the sampling points on transects, and crosses are the sampling points within deflation zone. X and Y axis are X- and Y-coordinate in RD ('Rijksdriehoekskoördinaten') system (unit m).

3.4.2 Vertical gradients in-situ pH at 0 – 10 cm depth

The vertical changes of in-situ pH are shown in Figure 18. Here a negative slope (i.e. dark green colour) means that top soil layers have higher pH than lower soil layers, whereas a positive slope means that top soil layers have lower pH than lower soil layers (thus indication of vertical pH gradient by acidification).

Around blowout 2, greater part of topsoil around the deflation zone has values close to 0 (i.e. no high positive values), indicating absence of an acidification gradient in the top soil. This is probably because of improved soil base status by the drift sand from the blowout. In the SW-transect of blowout 2 there is a spot with negative values, caused by recent sand deposition by another blowout SW of the deflation area of blowout 2. The other blowouts (8, 16, 21)

have several spots with high positive slopes, indicating presence of an acidification gradient in the top soil. At blowout 8 and 21 these areas with top soil acidification are located at one to several 10's of meters away from the border of the former deflation zone. Around blowout 16, top soil acidification occurred even in the areas close to the deflation zone.

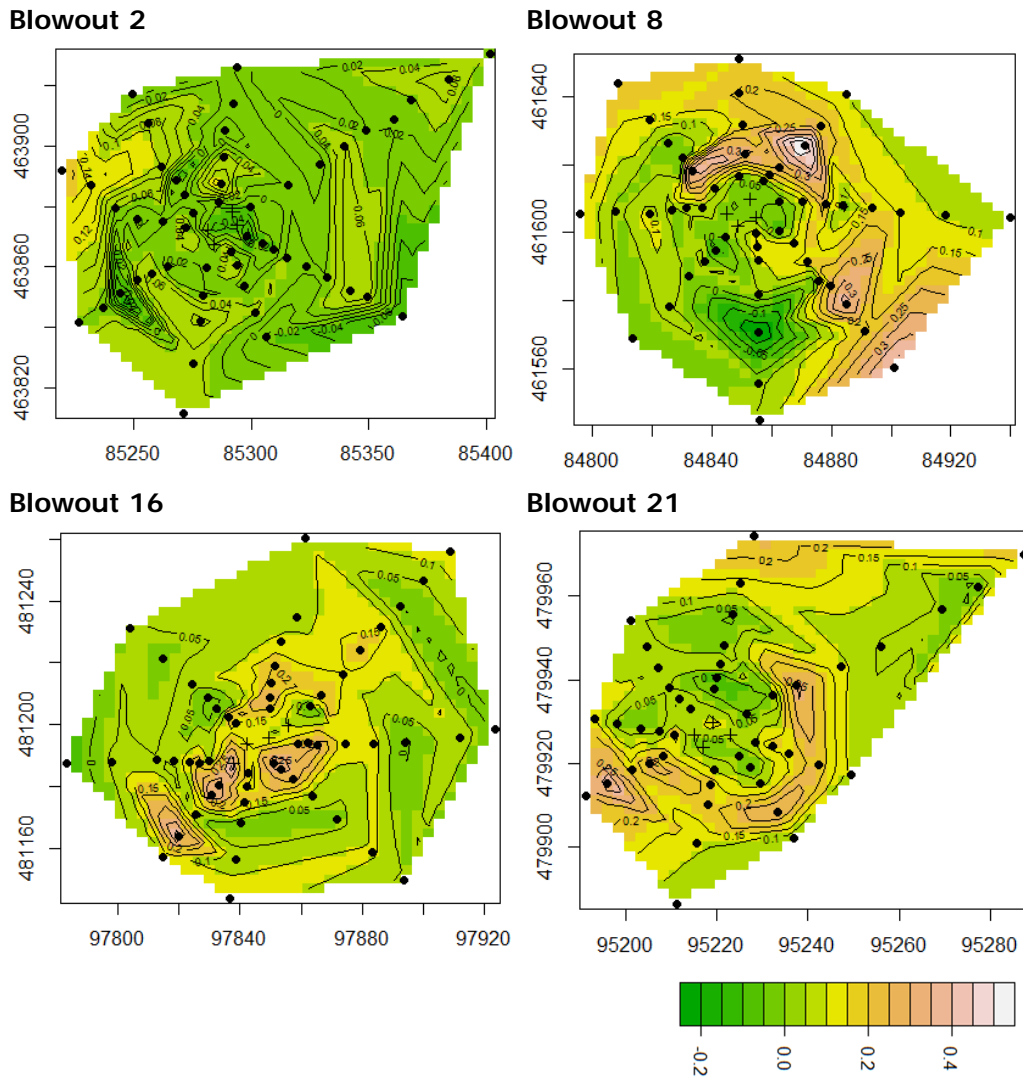


Figure 18. Vertical gradients of in-situ pH in the 0-10 cm topsoil (pH unit / cm). For a majority of the plots, pH values of 2.5, 5, 7.5, and 10cm depth were used to compute the slope of change. When top layers have higher pH than lower layers, the slope becomes negative (i.e. greener). Black dots are the sampling points on transects, and crosses are the sampling points within the deflation zone. X and Y axis are X- and Y-coordinate in RD ('Rijksdriehoekskoördinaten') system (unit m).

3.4.3 Decalcification depth

Decalcification depth (i.e. the shallowest depth where CaCO_3 was present in soil) is shown in Figure 19. All the deflations zones of the four blowout areas contained CaCO_3 in the topsoil. Around blowout 2, CaCO_3 was found in top soil (i.e. first cm of the mineral soil) in a large area around the deflation zone. In contrast, around blowout 8, 16, and 21, top soils containing CaCO_3

occurred in smaller zones. At blowout 2 the zone with a CaCO_3 -rich topsoil around the deflation zone was largest in transect NE, followed by transects S and SE. For blowout 8 this zone was largest in the NE-transect, but differences were small. At blowout 16 the zone with CaCO_3 -rich topsoil was broadest in the NE- and E-transect, and at blowout 21 in the NE-transect. At blowout 2 and 8 the parts with deeper decalcification had a decalcification depth of ca. 10-20 cm. For blowout 21 this is mostly ca. 10 to 25 cm and sometimes > 30 cm. Blowout 16 had deeper decalcification: often more than 30 cm.

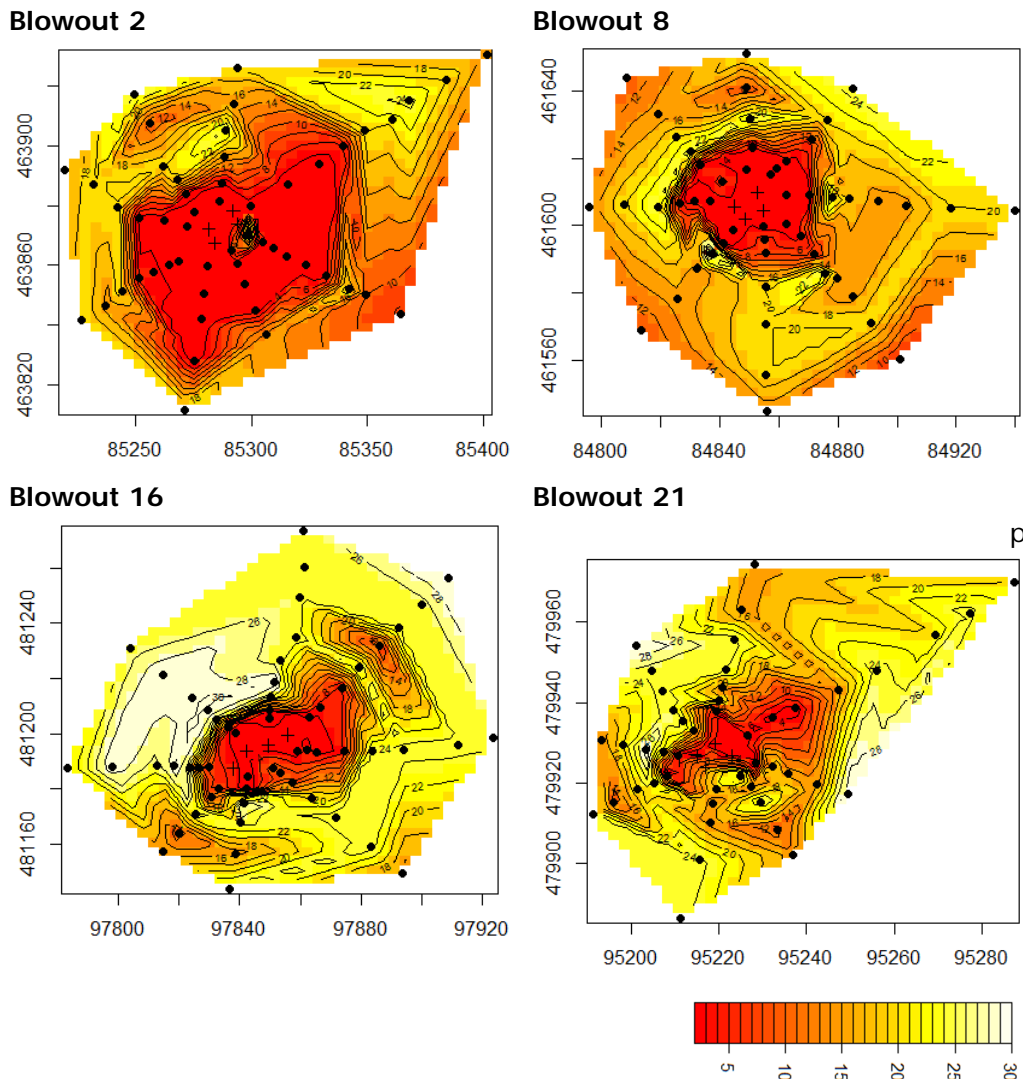


Figure 19. Contour map of decalcification depth (cm), made by linear interpolation of point data from soil sampling locations. Decalcification depth was defined as the middle depth of the shallowest soil layer where CaCO_3 was detected. Dots are the sampling points on transects, and crosses are the sampling points within deflation zone. X and Y axis are X- and Y-coordinate in RD ('Rijksdriehoekskoördinaten') system.

3.4.4 Estimated influenced area

Areas that are strongly and weakly influenced by sand deposition from the deflation area, judged from soil pH and CaCO_3 content (see Methods for more details), are roughly mapped in Figure 20. Blowout 2 has the largest zones, whereas blowout 8 and blowout 16 had intermediate sizes of influenced zones.

Blowout 21 had the smallest influenced zones (Table 3). Note that, for blowout 2, there is another deflation zone on the south side, which leads to overestimation of the influenced zone for blowout 2. Therefore, we also calculated the percentage of the influenced zone for blowout 2 by including the other deflation into the calculation of deflation zone (2' in Table 3). Still, blowout 2 had the largest relative influence of blowout than other blowouts. Mostly the weakly influenced zone is a little larger than the strongly influenced zone. However, at blowout 16 the weakly influenced zone is much larger than the strongly influenced zone.

Table 3. Areas of influenced zone of four blowouts. For blowout 2, an extra estimation was made with the assumption that another deflation zone on the South also contributed to the influenced area (2').

Blowout number	Deflation zone Size (m ²)	Strongly influenced zone Size (m ²)	Weakly influenced zone Size (m ²)	Influenced zone total	
				Size (m ²)	Percentage to size of deflation zone (%)
2	346.95	4483.21	819.60	5302.81	1528
2'	549.91	4280.25	819.60	5099.85	927
8	260.24	911.25	677.18	1588.43	610
16	397.21	362.55	1325.53	1688.08	425
21	224.90	189.59	139.50	329.08	146

*Sum of two deflation zones (the main deflation zone plus the deflation zone on the South)

Blowout 2



Blowout 8



Blowout 16



Blowout 21

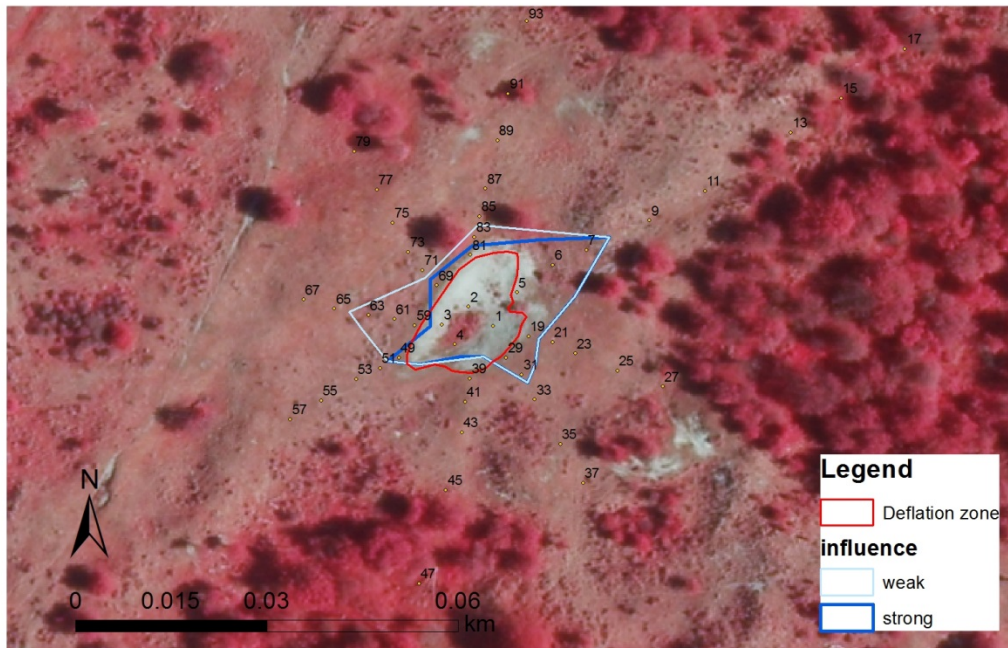


Figure 20. Strongly and weakly influenced areas by blowouts. The boundaries of deflation area (mapped with GPS in the field in 2015) are also drawn. Locations of each sampling points are shown with their plot ID number. Aerial photos of 2009 (for Meijendel) and 2011 (for Luchterduinen) are overlaid.

3.5 Vegetation

3.5.1 Vegetation cover

Vegetation cover within deflation zone and on NE transects are shown in Figure 21. Deflation zone of blowout 2 is only sparsely covered by herbs, whereas that of blowout 16 is highly covered either by herbs, mosses, or lichens. Deflation zones of blowout 8 and 21 are partly closed by vegetation. On the NE transect, most of the plots are fully covered by vegetation, mainly by mosses and lichens (of which mosses are most important). Only at the verge of the former deflation zone of blowout 2 and 21 there is a small zone with a low cover by mainly herbs.

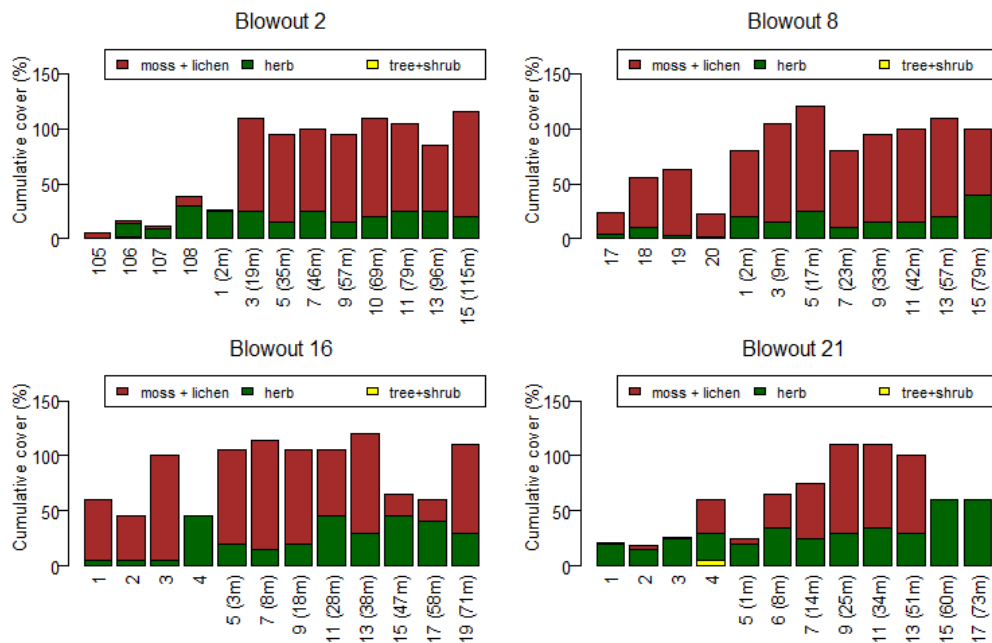


Figure 21. Cumulative cover of plants, categorized into functional groups (mosses+lichens, herbs, and trees and shrubs), of each plot. The four plots on the left side are within deflation zone. Rest of the plots are on NE transect, for which the distance between the plot and the boundary of the deflation zone are shown in bracket.

3.5.2 Ecological species group

Differences in species composition along NE transects are shown in terms of species number (Figure 22) and cumulative cover (Figure 23).

For all blowouts, species adapted to base-rich conditions (i.e. group 2 and 6) are slightly more abundant within deflation zone and close to the deflation zone in terms of species number (Figure 22). In terms of cover, the pattern was only visible for blowout 2 and blowout 8 (Figure 23). The effect of deposition of base rich sand seems to have an effect on species number of base rich species groups at a longer distance from the deflation area than on cover of these groups.

Species adapted to base-poor conditions (i.e. group 7) are more abundant in the NE transects than within deflation zone for all blowouts. The number of species of this group did not increase with the distance from the deflation

zone (Figure 22). However, for blowout 2, 8, and 16, cumulative cover of these species was higher in the plots further from the deflation area (Figure 23).

Note that species group 3 (dry dune grassland nutrient-poor) has in all transects a high cover. This is mainly due to the high cover of *Hypnum cupressiforme* var. *lacunosum*. A closer look at the zonation of specific species can reveal more insight in the vegetation gradients.

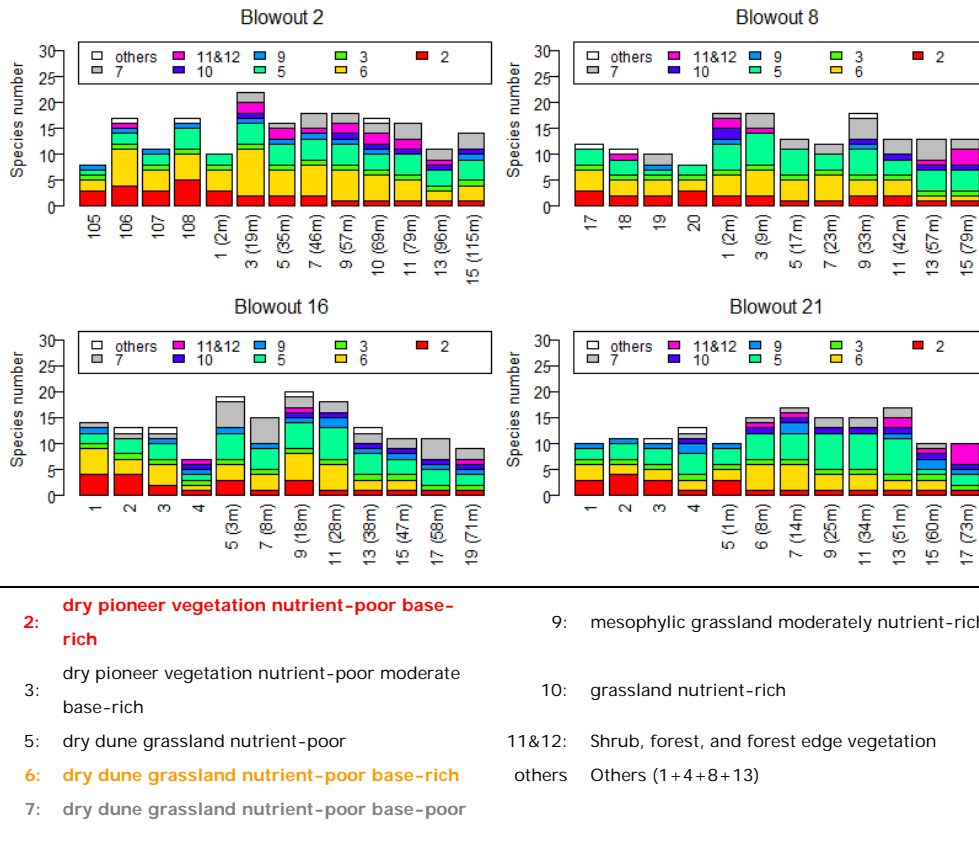


Figure 22. Number of species of each plot, split into ecological species groups. The four plots on the left side are within deflation zone. Rest of the plots are located at the NE transect, for which the distance between the plot and the boundary of the deflation zone are shown in bracket. We clumped four minor ecological groups (i.e. groups with less than 10 % cumulative cover in total) into a category 'others' (see Methods). Group 2 (red) and 6 (orange) are species typical for base-rich sites, whereas group 7 (pink) is species typical for base-poor sites.

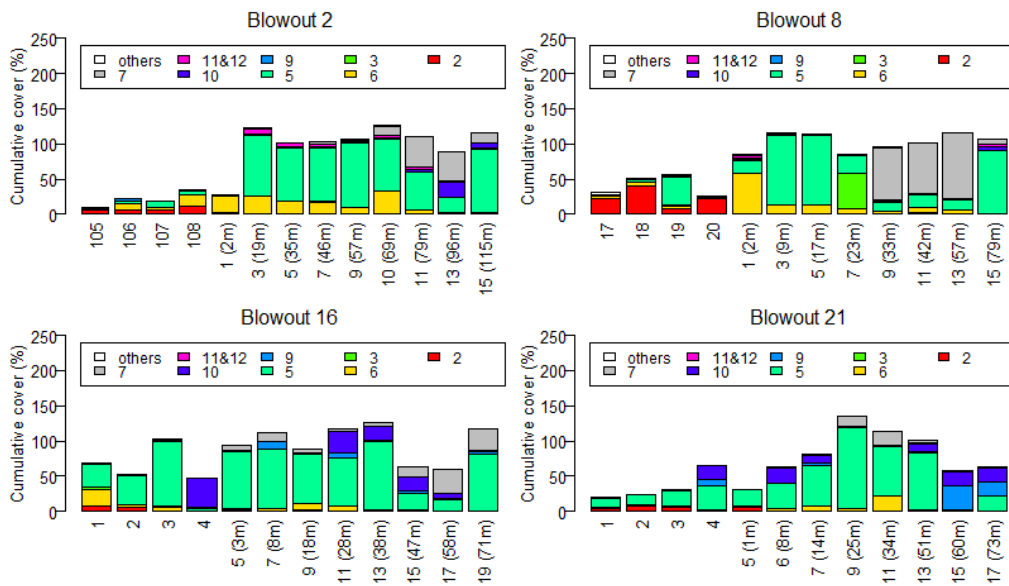


Figure 23. Cumulative cover of plant species of each plot, split into ecological species groups. The four plots on the left side are within deflation zone. Rest of the plots are located at the NE transect, for which the distance between the plot and the boundary of the deflation zone are shown in bracket. See Figure 22 for the description of each ecological species group.

3.5.3 Ellenberg acidity value

Weighted averages of Ellenberg acidity value are shown in Figure 24. In blowout 2 and 8, the average value is high in the deflation zone and in the transect close to the deflation zone, and decrease with distance from the deflation zone, indicating base rich conditions in the deflation zone and near this zone. In blowout 16 and 21 the deflation zone had lower acidity values than those in the other two blowouts. Also on the NE transect, the acidity values are low in blowout 16 and 21, and do not show a clear gradient with distance from the deflation zone (although in blowout 21 a slight decrease in acidity value can be seen).

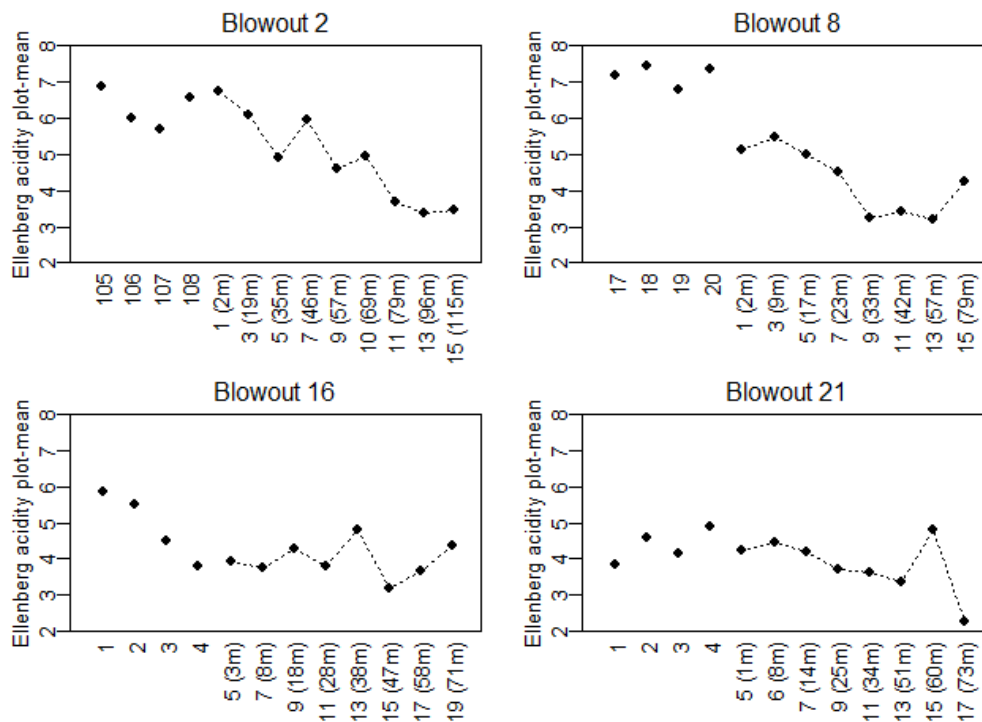


Figure 24. Plot-mean Ellenberg acidity value of the occurring species. The mean value was calculated by weighted by the cover of each species. The four plots on the left side are within deflation zone. Rest of the plots are on NE transect, for which the distance between the plot and the boundary of the deflation zone are shown in bracket. A higher Ellenberg acidity value means that the species is adapted to a higher pH range.

4 Synthesis of results

4.1 Effects on base chemistry of the top soil

In the four blowouts investigated the deposition of CaCO₃ containing sand from the deflation zones in the past has elevated the base status of the topsoil in the surrounding areas which were decalcified before the aeolian activity. Figure 25 illustrates there is a clear effect of the blowouts on the gradient of the topsoil pH. Around the former deflation zone the pH is higher than the pH of strongly acidified soils which were not or nearly affected by deposition of base rich sand. The spatial extent of this effect differs between the blowouts and also within the blowouts. In blowout 2 the spatial effect is largest, followed by blowout 8. This pattern is also shown by the differences in the area of strongly affected zones (Table 3). Differences in the area where soil base status is affected by sand deposition show no clear relationship with area of the blowout (Figure 26). Absence of a clear dependence on deflation area size might be caused by the small differences in deflation area size. All the four blowouts had also a small sized deflation area. Another confounding factor could be influence of drift sand from other deflation zones in the surroundings. For example, in blowout 2, there was an extra active deflation area in the neighbourhood, which could have contributed to the calculated size of influenced area. When the relative area of influenced zones (i.e. relative to deflation zone size) is related to the CaCO₃ content of the subsoil of the deflation area (10-15 cm depth), there seems to be a positive relationship: the higher the CaCO₃ content, the higher the relative size (Figure 27). This trend remains even when the deflation area of blowout 2 was corrected for the neighbouring extra deflation zone.

Elevation of the topsoil pH is most profound in NE to SE direction of the deflation zone, which is related to the prevailing wind direction (Figure 20). In the two blowouts of Luchterduinen (blowout 16 and 21) the effect was clearly most strong in NE direction. The effects of the blowouts on different directions were less visible in Meijendel.

Another factor influencing the observed patterns is the time lap between stabilization of the deflation zone and the moment of this study. Blowout 2 and 8 were stabilized 6-14 years ago, while blowout 16 was stabilized 14-25 years ago and blowout 21-25 years ago (Table 1). Moreover the deflation zones of blowout 2 and 8 are not completely stabilized and still showed weak aeolian activity. These differences could also add to a large area of the strongly affected zone in blowout 2 and 8.

Another factor to be looked at more closely is the difference in geomorphology and morphodynamics of the blowouts (Figure 4). The deflation zones of blowout 2, 8 and 16 are located on a dune top, while the deflation zone of site 21 was located at a low level in a dune zone with low dunes. This may partly explain the small area of influenced zone in blowout 21. Moreover the deflation zones of blowout 2 and 8 were eroded for several meters depth indicating much sand transport to the deposition area, while the other two

were eroded shallower and had probably much less sand transport. The strong sand transport of blowouts 2 and 8 might have attributed strongly to the area of the strongly affected zone. Therefore differences in the morphodynamics can have a dominant effect on the pattern of base chemistry. More detailed and quantitative analysis of sand transport and CaCO_3 contents in the sand will help understanding the processes which underlie the observed differences in influences of blowouts among sites.

At three of the four blowouts the weakly influenced zone was small in comparison with the strongly influenced zone. However at blowout 16, which had lowest CaCO_3 content in the deflation area, the weakly influenced zone was much larger than the strongly influenced zone. This is also reflected in the weak vertical gradients of the top soil pH, in contrast to the steep gradients in the other blowouts (Figure 25). Blowout 16 locates in the deeper decalcified inner dune zone, and the CaCO_3 content of the deflation zone was lowest of all blowouts. Deposition of moderate CaCO_3 rich sand, which occurred also relatively long ago (14-25 y), is reflected in 2015 in a weak elevation of the top soil pH compared to its local base line pH of strongly acidified soils.

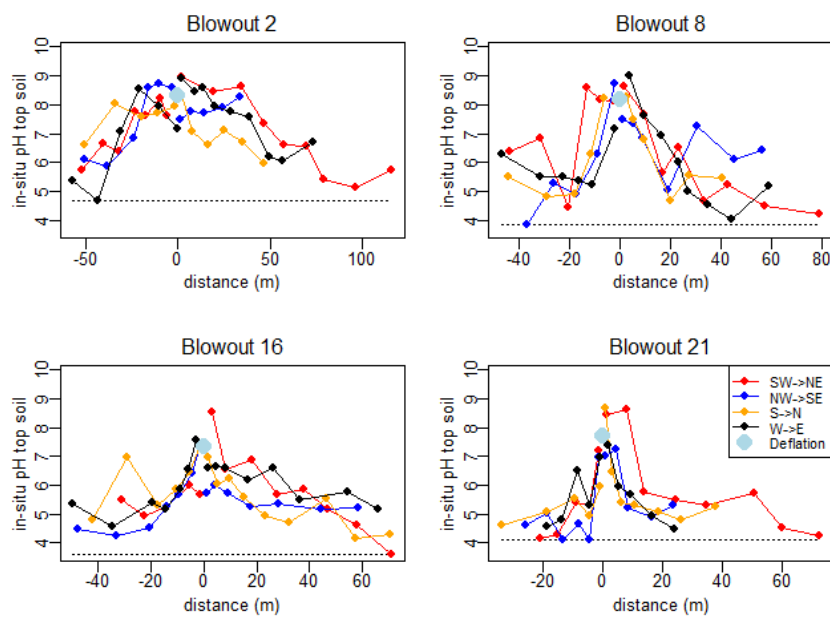


Figure 25. In-situ pH of the top soil (at 2.5 cm depth) in relation to the distance between the sampling point and the boundary of the deflation zone. Values are separately shown for each transect (SE→NE, NW→SE, S→N, and W→E), with the distances to the SW, NW, S, and W directions were expressed as negative. Note that for blowout 8 the names of transects are 45° shifted compared to the real direction in the field (i.e. 'NE transect' in the figure stretches to E direction in the field, 'E transect' in the figure stretches to SE direction in the field, etc.). Average values of in-situ pH within deflation zone (N=4) are also shown at the distance zero with light-blue circles. Baseline pH values, approximated as the lowest pH value of all transects around the blowout, are shown in dotted lines.

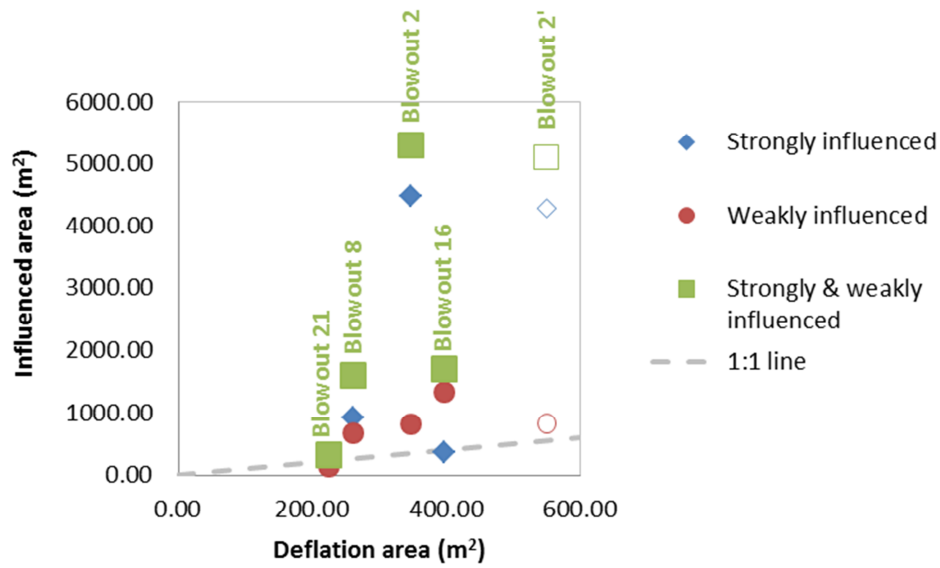


Figure 26: Relationship between the area of deflation size and the area of the influenced zone. Blowout 2 was also plotted for the corrected deflation area (i.e. the neighbouring extra deflation zone was summed up; 2' in Table 3) in non-filled symbols.

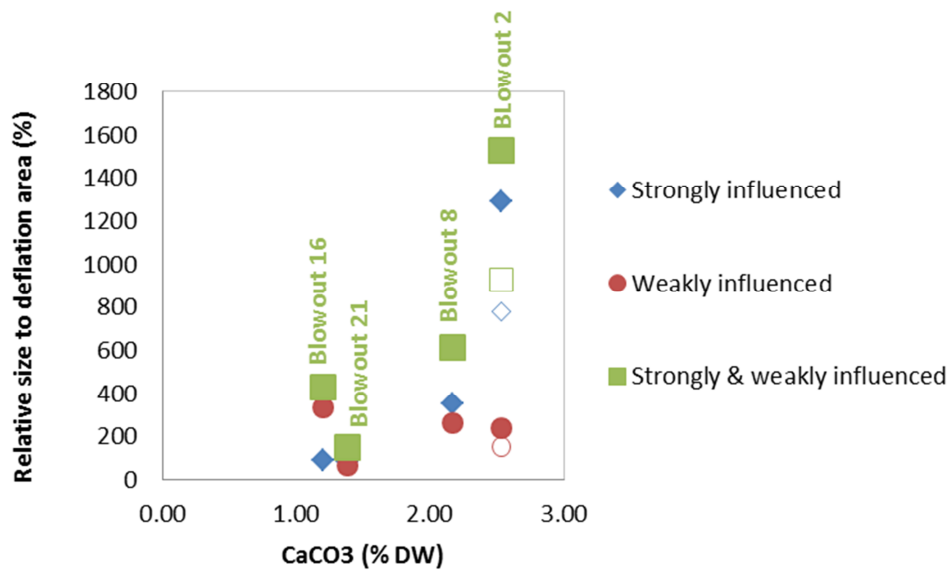


Figure 27: Relationship between the CaCO₃ content of the deflation zone at 10-15 cm depth and the relative size of the influenced zone to the deflation zone. The regression data apply for the strongly & weakly influenced zone. Blowout 2 was also plotted for the corrected deflation area (i.e. the neighbouring extra deflation zone was summed up; 2' in Table 3) in non-filled symbols.

4.2 Effects on vegetation

In the deflation zones species composition was clearly different from those on transects, due to the high CaCO₃ content, high pH of the topsoil, and succession stage. In deflation zone, the number of species typical for base-

rich pioneer vegetation and base-rich dune grassland was generally higher. However the dominance of these species in terms of cover was only evident in blowout 2 and 8, but not blowout 16 and 21. In the NE transect, these species were also more abundant in the plots close to the deflation zone, especially in blowout 2 and 8. Similarly, more rapid decrease in Ellenburg indicator values from deflation zone to NE transect was observed in blowout 2 and 8 compared to transect 16 and 21. These observations imply that high CaCO_3 content of the deflation zones (in blowout 2 and 8) has a positive effect on the cover of basiphilous species groups. When the gradients of species number and cover of base rich species are compared with the gradients of topsoil pH, the changes of species groups were more or less linked to the pH gradient (Figure 22 and Figure 23 compared with Figure 25). A drop in cover of basiphilous species coincide with a strong drop in pH values of the top soil. This means that base chemistry influenced the cover of basiphilous species. Note, however, that relatively high numbers of basiphilous species also occurred partly in the zones with a low pH, especially in blowout 2 and 8. This could be because of more sand deposition due to the difference in morphodynamics (as discussed in the previous section 4.1) as well as higher CaCO_3 contents in blowout 2 and 8. This might have caused a much higher acid buffer capacity in the top soil in the deposition zones, and therefore endurance of basiphilous species in these zones. The higher calciumcarbonate content may also be correlated to a less deep decalcification depth of the dune area. The decalcification rate (cm depth/y) is depended on the calciumcarbonate content (slower rate when CaCO_3 is higher). Therefore dune areas with a higher primary CaCO_3 content have a less deep decalcification depth than dune areas with a low primary CaCO_3 content. The background decalcification depth may also effect the vegetation patterns directly the pattern of basiphilous species. The decalcification depth of the dune area surrounding blowout 2 and 8 is less than those of blow 16 and 21. A more detailed analyses of special patterns of species and root depth traits of these species may give insight into the effect of deposition of base rich sand and of the background decalcification depth.

4.3 Conclusion

This study showed that base chemistry and vegetation of dune grassland soils adjacent to deflations zones of blowouts is still significantly affected after the blowout was stabilized for the greater part 14 to 25 years ago. These effects extend at a scale of ca. 10 to 80 m distance from the former deflation zone. Therefore reactivation of blowouts and subsequent stabilization after significant sand transport has occurred is suitable measure for restoration of base rich dune grasslands for a time scale of several decades. When the active period and period with a stabilized deflation zone are summed, survival time of base rich dune grassland species will be at least ca. 3-5 decades after aeolian activity started. This means natural and human-induced activation and subsequent stabilisation have much prospects for maintaining and restoring base rich dune grasslands at midterm timescale, and is a suitable measure for mitigating effects of soil acidification. Positive effects can be expected in sand deposition zones in existing dune grassland as well as in the stabilized deflation zones. The CaCO_3 content in the deflation zone (i.e. background content of the dune zone) and the magnitude of aeolian sand transport might influence the spatial extend of effects on topsoil base chemistry and species composition of the dune grassland in the deposition zone. The effects of these two factors have to be looked at more closely in future studies.

Table 4. Summary of characteristics of deflation zone and influence of blowouts on soil and vegetation in the surrounding area

Blowout nr.	Area	Dune zone	Distance to see (m)	Size of deflation zone	CaCO ₃ content in deflation zone* ¹	Vegetation development in deflation zone	Relative size of Influenced area* ²	Impact on top soil pH	Impact on depth of CaCO ₃ -contained soil	Impact on plant species composition
2	Meijendel	Middle dune	1560	347 m ² (550 m ² * ³)	ca. 2.5%	Sparse	1528 % (927 %* ³)	large	large	moderate
8	Meijendel	Inner dune	2580	260 m ²	ca. 2.2%	Half closed	610 %	moderate	moderate	moderate
16	Luchterduinen	Inner dune	4100	397 m ²	ca. 1.2%	Almost closed	425 %	small	small	weak
21	Luchterduinen	Middle dune	2270	224 m ²	ca. 1.4%	Half closed	146 %	moderate	small	weak

*¹: based on total Ca concentrations of 10-15cm depth, with an assumption that all Ca is present in CaCO₃.

*²: Relative to the size of the deflation zone. Strongly influenced and weakly influenced areas together.

*³: If the neighbouring extra deflation zone was summed up in the calculation of deflation zone.

5 References

Akima, H. (1978), A Method of Bivariate Interpolation and Smooth Surface Fitting for Irregularly Distributed Data Points, *ACM Transactions on Mathematical Software*, 4, 148-164.

Fujita, Y., and C. Aggenbach (2015), Effects of mowing, sod-cutting, and drift sand on development of soil and vegetation in Grey Dunes, Rapport KWR 2015.029., 126 pp, KWR.

Stuyfzand, P. J., S. M. Arens, A. P. Oost, and P. K. Baggelaar (2012), *Geochemische effecten van zandsuppleties in Nederland: Langs de kust van Ameland tot Walcheren 2012/OBN167-DK 150 pp*, Bosschap, bedrijfsschap voor bos en natuur.

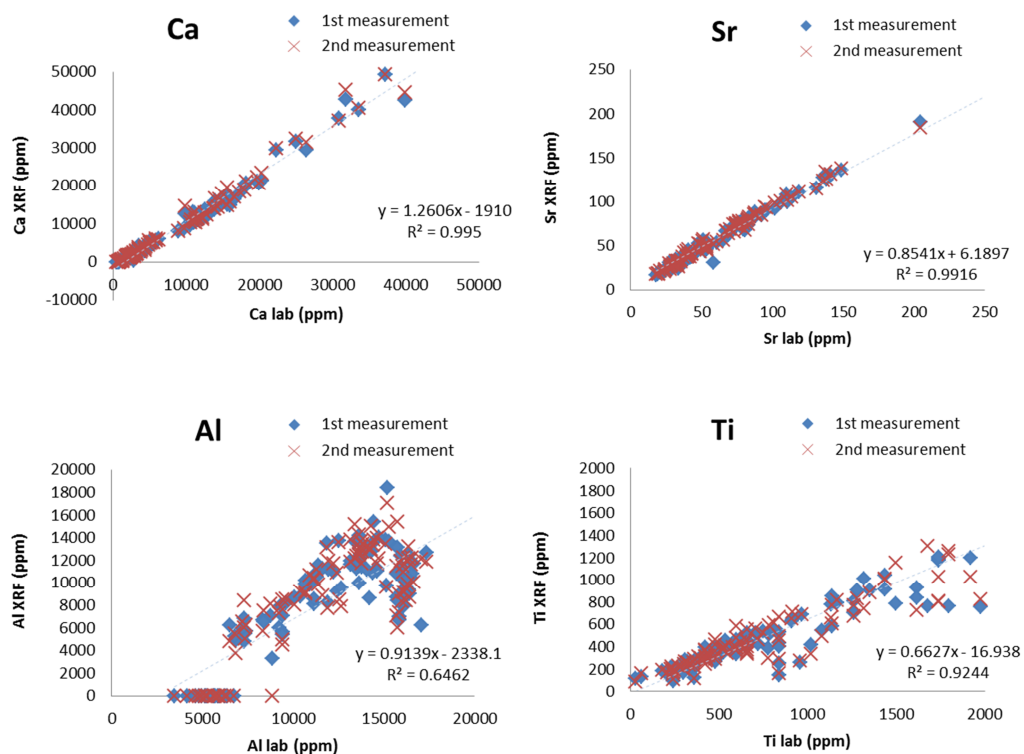
Van Delft, S. P. J. (2004), *Veldgids Humusvormen; Beschrijving, classificatie en interpretatie van humusvormen in het veld*, Alterra, Wageningen.

Appendix I XRF measurements

Reliability of handheld XRF measurements for estimating total amount of different elements was tested by comparing the element concentration estimated with XRF and those measured in 103 mineral soil samples, taken from foredune areas in the Netherlands [Stuyfzand *et al.*, 2012], was used for this test. The sampling depths ranged from 1 to 200 cm, with the majority of 10 cm (N=36), 30 cm (N=22) and 50 cm (N=28) depth.

Prior to the main test, we checked whether grinding affect the repeatability of the measurement results. For unground and hand-ground soil samples, the estimated concentrations differed considerably among multiple measurements for some elements, and especially for Ca. This indicates that soil is heterogeneous, and therefore fine machine-grinding is necessary to be able to obtain reliable estimates of element concentrations in these soil samples.

For the main test, 103 machine-ground soil samples were analysed. Each sample was measured twice with the XRF analyser. For 43 out of 103 soil samples, two subsamples were taken to conduct the first and the second measurements. Since 60 samples did not have enough amounts of soils to make two subsamples, the soil samples used for the first measurement was re-used for the second measurement after re-mixing the samples.



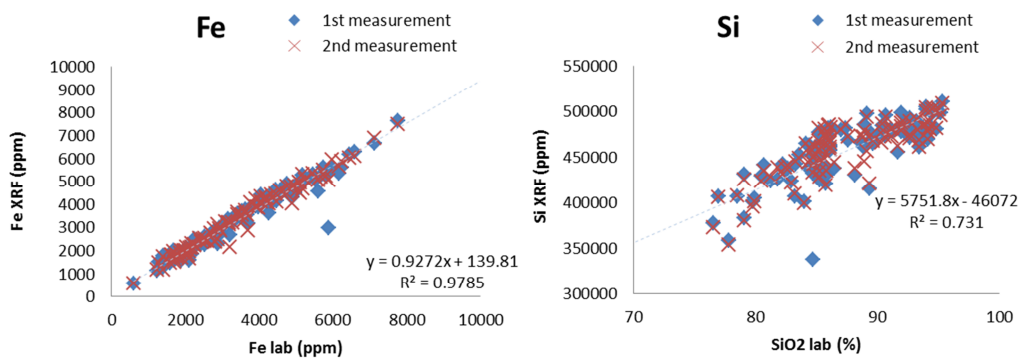


Figure 28. Comparison of two different methods, acid destruction (x-axis) and XRF (y-axis), to estimate total amount of elements (Ca, Sr, Al, Ti, Fe, and Si). Each of 103 soil samples was measured twice with a handheld XRF analyser. Linear regression models between the first measurement of XRF and acid destruction are shown.